# Accelerated Adaptive Fuzzy Optimal Control of Three Coupled Fractional-Order Chaotic Electromechanical Transducers

Shaohua Luo, Frank L. Lewis, *Fellow, IEEE*, Yongduan Song, *Fellow, IEEE*, and Hassen M. Ouakad, *Member, IEEE*

***Abstract*—In this article, we investigate the issue of the accelerated adaptive fuzzy optimal control of three coupled fractional-order chaotic electromechanical transducers. A small network where every transducer has the nearest-neighbor coupling configuration is used to form the coupled fractional-order chaotic electromechanical transducers. The mathematical model of the coupled electromechanical transducers with nearest-neighbors is established and the dynamical analysis reveals that its behaviors are very sensitive to external excitation and fractional order. In the controller design, the recurrent nonsingleton type-2 sequential fuzzy neural network (RNT2SFNN) with the transformation is designed to estimate unknown functions of dynamics system in the feedforward fuzzy controller, and it is constructed to approximate the critic value and actor control functions by using policy iteration (PI) in the optimal feedback controller. Meanwhile, the speed functions are employed to achieve accelerated convergence within a pregiven finite time and a tracking differentiator is used to solve the explosion of terms associated with traditional backstepping. The whole control strategy consists of a feedforward controller integrating with the RNT2SFNN, tracking differentiator, and speed function in the framework of the backstepping control and a feedback controller fusing with the RNT2SFNN and PI under an actor/critic structure to solve the Hamilton–Jacobi–Bellman equation. The proposed scheme not only guarantees the boundness of all signals and realizes the chaos suppression, synchronization, and accelerated convergence, but also minimizes the cost function. Simulations demonstrate and validate the effectiveness of the proposed scheme.**

***Index Terms*—Adaptive fuzzy optimal control, chaotic oscillation, coupled fractional-order electromechanical transducers, prescribed performance control, recurrent nonsingleton type-2 sequential fuzzy neural network (RNT2SFNN).**

Manuscript received August 29, 2019; revised February 26, 2020; accepted March 26, 2020. Date of publication April 3, 2020; date of current version July 1, 2021. This work was supported in part by the Science and Technology Planning Project of Guizhou Province ([2020]1Y274 and [2018]5781), in part by Young Scientific Talents of Education Department of Guizhou Province ([2018]111), and in part by the National Natural Science Foundation of China under Grant 61860206008, Grant 61773081, and Grant 61933012. *(Corresponding author: Yongduan Song.)*

Shaohua Luo is with the Key Laboratory of Advanced Manufacturing Technology, Ministry of Education, Guizhou University, Guiyang 550025, China, and also with UTA Research Institute, University of Texas at Arlington, Fort Worth, TX 76118 USA (e-mail: shluo@gzu.edu.cn).

Frank L. Lewis is with the UTA Research Institute, University of Texas at Arlington, Fort Worth, TX 76118 USA (e-mail: lewis@uta.edu).

Yongduan Song is with the State Key Laboratory of Power Transmission Equipment & System Security and New Technology, Chongqing Key Laboratory of Intelligent Unmanned Systems and School of Automation, Chongqing University, Chongqing 400044, China (e-mail: ydsong@cqu.edu.cn).

Hassen M. Ouakad is with the Department of Mechanical and Industrial Engineering, Sultan Qaboos University, Muscat 123, Oman (e-mail: houakad@squ.edu.om).

Color versions of one or more of the figures in this article are available online at https://ieeexplore.ieee.org.

Digital Object Identifier 10.1109/TFUZZ.2020.2984998

## I. Introduction

In recent years, the importance of complex networks with the interplay between the complexity of topology and dynamical properties of coupled units has been highlighted in the engineering [1], [2]. With the development of microelectromechanical systems ranging from mass sensing to electromechanical signal processing and computing, the topics such as the design, analysis, modeling, and control of coupled electromechanical systems have received recent attention and this tendency is increasing [2]–[9]. The electromechanical transducer, which can be applied to automotive industry, robot, consumer electronic products, and mobile phone industries, belongs to the moving coil electromechanical devices and its dynamical characteristics with related chaos and bifurcation can destroy system stability. Pérez-Molina and Perez-Polo [10] discussed nonlinear dynamics of the electromechanical transducer consisted of ferromagnetic mobile pieces under harmonic base oscillations. Ngueuteu *et al*. [11] investigated the dynamics and synchronization of two distributed coupled electromechanical transducers. The works are confined to modeling and analysis of integer-order electromechanical transducers. Hereafter, Ngueuteu and Woafo [3] further investigated the dynamics and synchronization analysis of the coupled electromechanical transducer, wherein the fractional characteristics of the capacitors were incorporated. Aghababa [12] set up a fractional robust sliding mode controller to stabilize an electrostatic and electromechanical transducer. Unfortunately, this scheme is excessively dependent on known dynamics and matched conditions without the generic coupling configuration, and it does not get involved in issues such as the prescribed performance control and optimal control.

To compensate for the effects of unknown dynamics, many useful approximators, such as the fuzzy logic, neural network, and observer and Legendre polynomial, are integrated with stabilization control methods [13]–[20]. It is well known that adaptive backstepping control methods fusing with the mentioned approximators are widely used to control uncertain systems due

to favorable advantages [13], [14], [21], [22]. Some researchers applied the idea of backstepping to control fractional-order nonlinear systems [23]–[28]. However, the dynamics of the controlled objects under these schemes are known in advance and the explosion of terms is unavoidable as the order of the system increases in [23] and [24]. In addition, the optimality associated with the Hamiltonian function is neglected. Direct derivation for virtual control inputs can result in repeated differentiation and the quantity of weights matches up with fuzzy basis functions under the large computation burden in [25]–[28]. Otherwise, the optimality of controllers is not considered. A first-order filter is introduced to tackle the complexity growth problem [22]. Nevertheless, its filter precision is poorer compared with the tracking differentiator (TD). The prescribed performance control is a good choice to accelerate the convergence rate and achieve the given performance specifications [29], [30]. But this approach relies heavily on initial conditions. Song and Zhao [31] developed an accelerated adaptive control method for a class of nonlinear uncertain systems. But its model is no mention of unknown nonlinear functions and it only applies to integer-order systems due to the complexity of fractional calculus. Therefore, how to develop a prescribed performance fuzzy backstepping control scheme for the fractional-order coupled nonlinear systems is still an open issue.

Optimal control has attracted increasing attention since it has consumed fewer resources [14], [22], [32]–[36]. The core challenge of the optimal control is to solve the underlying Hamilton–Jacobi–Bellman (HJB) equation and minimize the structured cost index. To tackle insufficient knowledge of system dynamics and poor approximate accuracy, the neural network as a function approximator is chosen to implement the PI algorithm in [32]–[35]. It is worth noting that there exists local minima, open analysis, and poor convergence issues. To solve these problems, Liu *et al*. [14] designed a fuzzy approximation-based adaptive backstepping optimal controller for a class of nonlinear discrete-time systems. Li *et al*. [17] discussed the observer-based adaptive fuzzy fault-tolerant optimal control problem for SISO nonlinear systems. Sun and Liu [22] proposed a distributed fuzzy adaptive backstepping optimal control method for nonlinear multimissile guidance systems with input saturation. They incorporated the optimal control idea into adaptive backstepping control. However, these methods are invalid for fractional-order coupled nonlinear systems due to the complexity of the fractional derivative. Meanwhile, the issues such as the given performance specifications, time delays, chaos suppression, and complexity growth problem are not involved. Besides, a network of coupled fractional-order electromechanical transducers can model parallel operating systems, intestinal signals, colorectal myoelectrical activities, and pattern generators, which is totally different from a class of nonlinear systems mentioned above.

Motivated by the aforementioned works, we propose an accelerated adaptive fuzzy optimal control scheme for three coupled fractional-order electromechanical transducers. The real control strategy is made up of a feedforward controller fusing with the recurrent nonsingleton type-2 sequential fuzzy neural network (RNT2SFNN), TD, and speed function in the framework of the backstepping control and a feedback controller engaging with the RNT2SFNN and PI under an actor/critic structure. The main contributions of our article can be summarized as follows.

First, a small network of electromechanical transducers and its mathematical model, which owns the nearest-neighbor coupling configuration, are proposed with considering the fractional-order characteristics of the velocity and capacitor in contrast with [3], [37]. It can increase memory properties and design freedoms and facilitate later technological exploitation in industrial chains.

Second, we introduce a fuzzy optimal control method into the accelerated backstepping control, which broadens the application scope of the fractional-order backstepping control. Comparing with [23], [25]–[28], the key issues such as the optimality of the control and accelerated convergence within the finite time are not involved at all. Meanwhile, a network of coupled electromechanical transducers is very different from a class of nonlinear systems, and how to effectively control it is a challenging and very significant issue.

Finally, the works in [38]–[42] are confined to adaptive optimal control of single integer-order and uncoupled system. And the accelerated convergence and transformations associated with fuzzy logic and neural network, which decide the controller performance, are not taken into consideration. By contrast, our proposed scheme can guarantee the boundness of all signals and minimize the cost function. Meanwhile, it achieves the goals of chaos suppression, synchronization, and accelerated convergence.

The rest of the article is organized as follows. Section II presents the problem formulation and preliminaries. Sections III and IV give the design processes of the feedforward fuzzy controller and an adaptive optimal feedback controller. Section V presents the stability analysis. Section VI provides and discusses the simulation results. Finally, Section VII concludes the article.

## II. Optimal Control Formulation and Preliminaries

In Section II-A, we develop the dynamical model for coupled fractional-order chaotic electromechanical transducers. Then, in Section II-B, we provide a novel optimal control formulation that is seen to significantly improve the performance.

### A. Modeling of Coupled Electromechanical Transducers

A single electromechanical transducer usually consists of a linear mechanical oscillator and a Duffing-Quintic electrical oscillator, wherein two oscillators interact with each other by a magnetic flux of density. The mechanical oscillator is composed of a moving beam that can oscillate along the $z$-axis. The electrical oscillator is made up of the resistance, nonlinear capacitor, inductor, and sinusoidal voltage source. Based on Newton's second law and Kirchhoff's law, the kinetic equation of a single fractional-order electromechanical transducer can be expressed as [3], [37]

$$\begin{cases} L^C \mathscr{D}_{0,t}^{2\alpha} q_i + R^C \mathscr{D}_{0,t}^{\alpha} q_i + \frac{1}{C_0} q_i + a_3 q_i^3 + a_5 q_i^5 \\ \quad + lB^C D \mathscr{D}_{0,t}^{\alpha} z_i - v_0 \cos \omega' \tau = \nu_i = 0 \\ m^C \mathscr{D}_{0,t}^{2\alpha} z_i + \eta^C \mathscr{D}_{0,t}^{\alpha} z_i + k z_i - lB^C \mathscr{D}_{0,t}^{\alpha} q_i = 0, \quad i = 1, 2, 3 \end{cases} \tag{1}$$

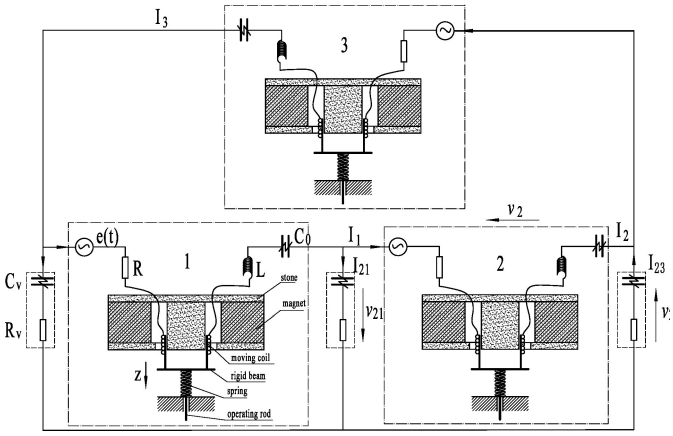


Fig. 1. Schematic diagram of three coupled fractional-order electromechanical transducers.

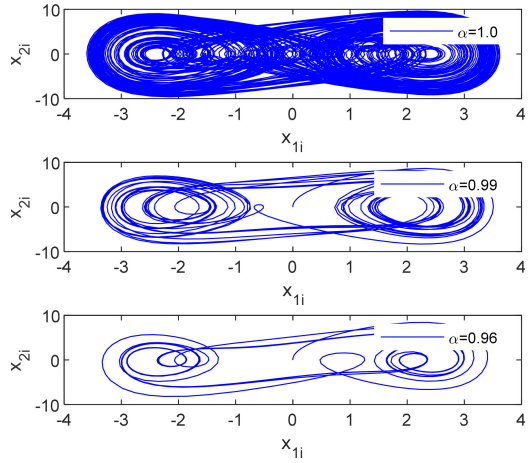


Fig. 2. Phase diagrams between $x_{1i}$ and $x_{2i}$ under $\kappa_1 = \kappa_2 = 0.1$.

where $L$, $R$, $C_0$, $v_0$, and $\omega'$ represent the inductor, resistance, capacitor, amplitude, and frequency, respectively; $a_3$ and $a_5$ are the system coefficients; $\alpha$ and $C$ denote the fractional order satisfying $0 < \alpha < 1$ and Caputo fractional derivative; and $m$, $\eta$, $k$, $l$, $B$, and $\nu_i$ denote the mass, viscous friction coefficient, stiffness coefficient, length of the moving coil, magnetic flux of density, and voltage of the $i$th electromechanical transducer, respectively.

A network of electromechanical systems plays an important part in technological exploitations for industrial chains and it operates in parallel mode for loading in assembly line works and scaling up manufacturing processes. This network can mix different substances and realize the transmission of multiple signals, and it is also used to investigate the possibility of simultaneous multimode oscillations. So we create a small network made up of three identical electromechanical transducers. Every transducer has the nearest-neighbor coupling configuration by the aid of the series-association of the capacitor and resistance. The schematic diagram of three coupled electromechanical transducers is shown in Fig. 1. There exist the following relations among three identical electromechanical transducers:

$$\nu_i = -\nu_{i,i-1} - \nu_{i,i+1}, \quad I_{i,i-1} = I_i - I_{i-1} \tag{2}$$

where $I_i$, $I_{i,j}, j = i-1$, and $\nu_{i,j}, j = i-1$ or $i+1$ denote the currents through the $i$th electromechanical transducer, the currents crossing the branch, and the voltages of the branch coupling.

It is gotten as $\nu_{i,j} = \frac{1}{C_v} q_{i,j} + R_v I_{i,j} = \frac{1}{C_v}(q_i - q_j) + R_v(I_i - I_j)$, where $q_{i,j}$, $C_v$, and $R_v$ represent the coupled capacitor charge, capacitor, and resistance of the branch coupling, respectively. Then it has

$$\nu_i = \frac{1}{C_v}\left(q_{i-1} - 2q_i + q_{i+1}\right) + R_v\left({}^C D\mathscr{D}^{\alpha}_{0,t} q_{i-1} - 2\,{}^C D\mathscr{D}^{\alpha}_{0,t} q_i + {}^C\mathscr{D}^{\alpha}_{0,t} q_{i+1}\right). \tag{3}$$

With (1), the kinetic equation of three nearest-neighbor coupled fraction-order electromechanical transducers is derived as

$$\begin{cases} L\,{}^C\mathscr{D}^{2\alpha}_{0,t} q_i + R\,{}^C D\mathscr{D}^{\alpha}_{0,t} q_i + q_i/C_0 + a_3 q_i^3 + a_5 q_i^5 \\ \quad + lB\,{}^C\mathscr{D}^{\alpha}_{0,t} z_i - v_0 \cos\Omega\tau \\ = \left(q_{i-1} - 2q_i + q_{i+1}\right)/C_v + R_v \\ \quad \times \left({}^C\mathscr{D}^{\alpha}_{0,t} q_{i-1} - 2\,{}^C\mathscr{D}^{\alpha}_{0,t} q_i + {}^C\mathscr{D}^{\alpha}_{0,t} q_{i+1}\right) \\ m\,{}^C\mathscr{D}^{2\alpha}_{0,t} z_i + \eta\,{}^C\mathscr{D}^{\alpha}_{0,t} z_i + k z_i - lB\,{}^C\mathscr{D}^{\alpha}_{0,t} q_i = 0. \end{cases} \tag{4}$$

Define the dimensionless variables $x_{1i} = q_i/Q_0 \in \mathbb{R}$ with the reference charge $Q_0$ of the capacitor, $x_{3i} = z/l \in \mathbb{R}$ and $t = \omega_e \tau$ with $\omega_e = (LC_0)^{-\frac{1}{2}}$. By adding with control inputs for (4), the nondimensionalized equation of three nearest-neighbor coupled fraction-order electromechanical transducers is written as

$$\begin{cases} {}^C\mathscr{D}^{\alpha}_{0,t} x_{1i} = x_{2i} \\ {}^C\mathscr{D}^{\alpha}_{0,t} x_{2i} = -\gamma_1 x_{2i} - x_{1i} - \beta_1 x_{1i}^3 - \beta_2 x_{1i}^5 \\ \quad -\zeta_1 x_{4i} + E_0 \cos\omega t \\ \quad +u_{2i} + \kappa_1\left(x_{1(i-1)} - 2x_{1i} + x_{1(i+1)}\right) \\ \quad +\kappa_2\left(x_{2(i-1)} - 2x_{2i} + x_{2(i+1)}\right) \\ {}^C\mathscr{D}^{\alpha}_{0,t} x_{3i} = x_{4i} \\ {}^C\mathscr{D}^{\alpha}_{0,t} x_{4i} = -\gamma_2 x_{4i} - \omega_2^2 x_{3i} + \zeta_2 x_{2i} + u_{4i} \end{cases} \tag{5}$$

where $\gamma_1 = \frac{R}{L\omega_e}$, $\gamma_2 = \frac{\eta}{m\omega_e}$, $\beta_1 = \frac{a_3 Q_0^2}{L\omega_e^2}$, $\beta_2 = \frac{a_5 Q_0^4}{L\omega_e^2}$, $\omega = \frac{\omega'}{\omega_e}$, $\zeta_1 = \frac{l^2 B}{LQ_0\omega_e}$, $\zeta_2 = \frac{BQ_0}{m\omega_e}$, $\omega_2^2 = \frac{k}{m\omega_e^2}$, $\kappa_2 = \frac{R_v}{L\omega_e}$, $E_0 = \frac{v_0}{LQ_0\omega_e}$, and $\kappa_1 = C_0/C_v$ denote dimensionless parameters, and $u_{2i} \in \mathbb{R}$ and $u_{4i} \in \mathbb{R}$ are the control inputs needed to be chosen.

The system parameters of a single electromechanical transducer are given as $\gamma_1 = 0.2$, $\gamma_2 = 0.1$, $\beta_1 = 0.9$, $\beta_2 = 0.1$, $\zeta_1 = 0.01$, $\zeta_2 = 0.05$, $\omega_2 = 1.2$, $\omega = 0.85$, and $E_0 = 23.5$ [3], [37]. $\kappa_1$ and $\kappa_2$ denote capacitive and resistive coupled coefficients. Besides, $\kappa_2$ involves the dissipative coupling that can strengthen the exponential decay of the transverse perturbation. Fig. 2 and 3 reveal that three coupled electromechanical transducers have various dynamical states and behaviors such as chaotic oscillations under the different fractional orders. Fig. 4 shows the phase diagrams for external excitations under the nearest-neighbor coupling configuration. It is obvious that the

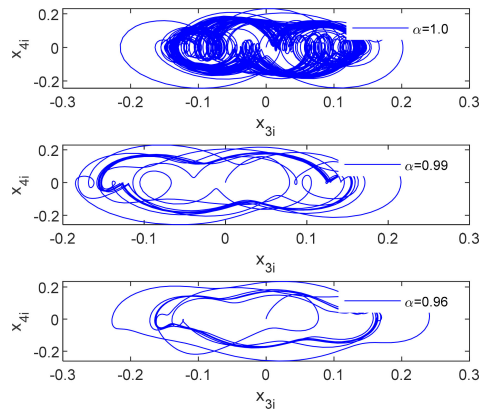


Fig. 3. Phase diagrams between $x_{3i}$ and $x_{4i}$ under $\kappa_1 = \kappa_2 = 0.1$.

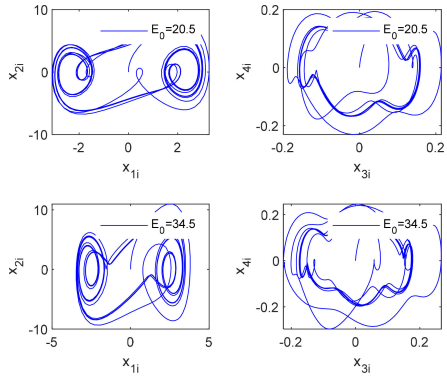


Fig. 4. Phase diagrams for the external excitation under $\kappa_1 = \kappa_2 = 0.1$ and $\alpha = 0.99$.

dynamical behaviors of the system are very sensitive to parameter variations. It is noteworthy that the chaotic oscillation can lead to system instability in its running process without effective schemes.

*Remark 1:* If $\kappa_1 = \kappa_2 = 0$ and $\alpha = 1$, three coupled fractional-order electromechanical transducers retrograde into a single general electromechanical transducer. In contrast with [3], [37], we consider the fractional-order characteristic of the velocity for the mobile beam, which increases the memory properties and design freedoms. Meanwhile, it is expanded to three coupled electromechanical transducers through the branch coupling configuration.

There exists the time delays for system states $x_{1i}$ and $x_{3i}$ in the work process, especially in the cases of low rate start and reverse motion. Then the mathematical equation of three coupled fractional-order electromechanical transducers is given as follows:

$$\begin{cases} {}^{C}\mathscr{D}^{\alpha}_{0,t}x_{1i} = x_{2i} \\ {}^{C}\mathscr{D}^{\alpha}_{0,t}x_{2i} = -\gamma_1 x_{2i} - \zeta_1 x_{4i} + E_0 \cos \omega t \\ \quad + h_{2i}\left(x_{1i}\left(t-\tau_{1i}\right)\right) \\ +u_{2i} + \kappa_1\left(x_{1(i-1)} + x_{1(i+1)}\right) \\ \quad + \kappa_2\left(x_{2(i-1)} - 2x_{2i} + x_{2(i+1)}\right) \\ {}^{C}\mathscr{D}^{\alpha}_{0,t}x_{3i} = x_{4i} \\ {}^{C}\mathscr{D}^{\alpha}_{0,t}x_{4i} = -\gamma_2 x_{4i} + \zeta_2 x_{2i} + h_{4i}\left(x_{3i}\left(t-\tau_{3i}\right)\right) + u_{4i} \end{cases} \tag{6}$$

where $h_{4i}(x_{3i}(t-\tau_{3i})) = -\omega_2^2 x_{3i}(t-\tau_{3i})$ and $h_{2i}(x_{1i}(t-\tau_{1i})) = -x_{1i}(t-\tau_{1i}) - \beta_1 x_{1i}^3(t-\tau_{1i}) - \beta_2 x_{1i}^5(t-\tau_{1i}) - 2\kappa_1 x_{1i}(t-\tau_{1i})$ denote the time-varying time delay items, and $\tau_{ji} = \tau_{ji}(t), j = 1, 3$.

### B. Preliminaries and Control Formulations

*Definition 1 [43], [44]:* The Caputo fractional derivative for a real function $F(t)$ can be written as

$${}^{C}\mathscr{D}^{\alpha}_{a,t}F(t) = \frac{1}{\Gamma(n-\alpha)}\int_a^t (t-\tau)^{n-\alpha-1}\left(\frac{d}{dt}\right)^n F(\tau)\, d\tau \tag{7}$$

where $\Gamma(n-\alpha)$ denotes the Gamma function and is equal to $\int_0^\infty e^{-t}t^{n-\alpha-1}dt$, $n-1 < \alpha < n$ and $n \in \mathbb{N}_+$.

*Definition 2 [43], [44]:* The Riemann–Liouville (RL) fractional integral for $F(t)$ is defined as

$${}^{RL}\mathscr{I}^{\alpha}_{a,t}F(t) = \frac{1}{\Gamma(\alpha)}\int_a^t (t-\tau)^{\alpha-1}F(\tau)\, d\tau. \tag{8}$$

*Lemma 1 [44]:* If $y(x) \in C^n[a,b]$ and $\alpha > 0$, it has the following equality:

$${}^{RL}I^{\alpha}_{a,t}\left({}^{C}\mathscr{D}^{\alpha}_{a,t}y(x)\right) = y(x) - \sum_{k=0}^{n-1}\frac{y^{(k)}(a)}{k!}(x-a)^k. \tag{9}$$

*Assumption 1:* The reference signals $x_{L_j} \in \mathbb{R}, j = 1, 3$ and its derivatives are continuous and available.

*Assumption 2:* There are unknown positive functions $q_{2j}$ and $q_{4j}$ satisfying

$$\begin{cases} |h_{2i}(x_{1i}(t-\tau_{1i}))| \le \sum_{j=1}^{2}|S_{ji}|\, q_{2j}(x_{1i}, x_{2i}) \\ |h_{4i}(x_{3i}(t-\tau_{3i}))| \le \sum_{j=3}^{4}|S_{ji}|\, q_{4j}(x_{3i}, x_{4i}) \end{cases} \tag{10}$$

where the accelerated error variables $S_j, j = 1, \ldots, 4$ are given later.

*Remark 2:* The Assumption 1 is customary in most of literatures of trajectory tracking. In contrast with [45], the time delay terms in Assumption 2 include the whole state variables that can extend its application.

*Assumption 3:* The terms of the time-varying time delays $\tau_{1i}(t)$ and $\tau_{3i}(t)$ satisfy the following inequalities:

$$0 \le \tau_{ji}(t) \le \tau_{\max}, \quad {}^{C}\mathscr{D}^{\alpha}_{a,t}\tau_{ji}(t) \le \bar{\tau}_{\max} < 1, \quad j = 1, 3 \tag{11}$$

where $\tau_{\max}$ and $\bar{\tau}_{\max}$ denote the known constants.

Introduce the infinite horizon cost function [32], [34], [42]

$$J_i = \int_0^\infty \left(Q_i(S_i(\tau)) + U_i(\tau)^T R_i U_i(\tau)\right)d\tau \tag{12}$$

where $Q_i(\mathbf{S}_i) > 0$, $R_i \in \mathbb{R}^{N\times N}$, $\mathbf{S}_i$, and $U_i$ represent the penalty function, symmetric positive definite, tracking error, and control input, respectively.

The optimal control problem of this article is formulated: Given three coupled fractional-order chaotic electromechanical transducers (6), the admissible control policies $u_{ji}$, $j = 2, 4$, and the cost function (12), find an accelerated adaptive fuzzy optimal control policy such that all signals in the closed-loop system are bounded, the purposes of the chaos suppression, synchronization, and accelerated convergence are achieved, and the cost function (12) is minimized.

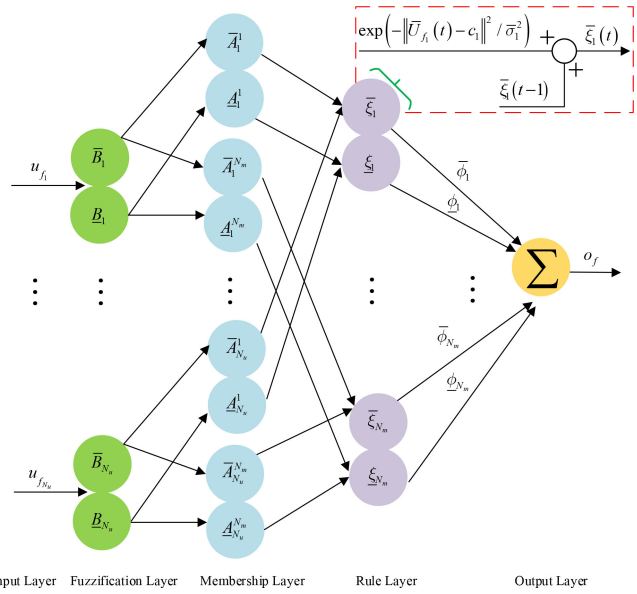


Fig. 5. Schematic diagram of the RNT2SFNN.

## III. Feedforward Fuzzy Controller Design

### A. Recurrent Nonsingleton Type-2 Sequential Fuzzy Neural Network

The RNT2SFNN [46], which is powerful in function learning and approximating capacity, combines advantages of the fuzzy system and radial basis function neural network, and consists of five layers such as input, fuzzification, membership, rule, and output layers. Fig. 5 shows the schematic diagram of the RNT2SFNN. Its output process is summarized as follows.

1) Compute upper membership $\bar{\mu}_{\tilde{A}_j^i}$ and lower membership $\underline{\mu}_{\tilde{A}_j^i}$

$$\bar{\mu}_{\tilde{A}_j^i} = \exp\left(\frac{-\left(\bar{u}_{f_j^i}(t) - c_{\tilde{A}_j^i}\right)^2}{\bar{\sigma}^2_{\tilde{A}_j^i}}\right), \quad \underline{\mu}_{\tilde{A}_j^i} = \exp\left(\frac{-\left(\underline{u}_{f_j^i}(t) - c_{\tilde{A}_j^i}\right)^2}{\underline{\sigma}^2_{\tilde{A}_j^i}}\right), \quad i = 1, \ldots, N_m, \quad j = 1, \ldots, N_u \tag{13}$$

with

$$\bar{u}_{f_j^i} = \frac{\bar{\sigma}^2_{\tilde{B}_j} c_{\tilde{A}_j^i} + \bar{\sigma}^2_{\tilde{A}_j^i} u_{f_j}}{\bar{\sigma}^2_{\tilde{B}_j} + \bar{\sigma}^2_{\tilde{A}_j^i}}$$

and

$$\underline{u}_{f_j^i} = \frac{\underline{\sigma}^2_{\tilde{B}_j} c_{\tilde{A}_j^i} + \underline{\sigma}^2_{\tilde{A}_j^i} u_{f_j}}{\underline{\sigma}^2_{\tilde{B}_j} + \underline{\sigma}^2_{\tilde{A}_j^i}}$$

where $c_{\tilde{A}_j^i}$, $u_{f_j}$, $\bar{u}_{f_j^i}$, and $\underline{u}_{f_j^i}$ represent the center, input, upper input, and lower input of the membership function (MF), respectively, $\bar{\sigma}_{\tilde{A}_j^i}$ and $\bar{\sigma}_{\tilde{B}_j}$ denote the upper widths of the MF, and $\underline{\sigma}_{\tilde{A}_j^i}$ and $\underline{\sigma}_{\tilde{B}_j}$ are the lower widths of the MF.

2) Knowledge base for the RNT2SFNN consists of a series of fuzzy IF–THEN rules

If $u_{f_1}$ is $\tilde{A}_1^l$ and $\cdots$ and $u_{f_{N_u}}$ is $\tilde{A}^l_{n_{N_u}}$, then

$$o_f \in \left[\underline{\phi}_l, \bar{\phi}_l\right], \quad l = 1, \ldots, N_u \tag{14}$$

where $\tilde{A}_j^l, j = 1, \ldots, N_u$ denote the $l$th Gaussian type-2 MF for the $j$th input.

The upper and lower firing degrees can be expressed as

$$\begin{cases} \bar{\xi}_i(t) = r\bar{\xi}_i(t-1) + \exp\left(-\left\|\bar{U}_{f_i}(t) - c_i\right\|^2/\bar{\sigma}_i^2\right) \\ \underline{\xi}_i(t) = r\underline{\xi}_i(t-1) \\ \quad + \exp\left(-\left\|\underline{U}_{f_i}(t) - c_i\right\|^2/\underline{\sigma}_i^2\right), \quad i = 1, \ldots, N_m \end{cases} \tag{15}$$

where $\bar{\xi}_i(t-1)$ and $\underline{\xi}_i(t-1)$ denote the upper and lower firing degrees of the $i$th rule at previous sample time, $r$ is a design parameter,

$$c_i \equiv \left[c_{\tilde{A}_1^i}, \ldots, c_{\tilde{A}_{N_u}^i}\right]^T, \bar{U}_{f_i} \equiv \left[\bar{u}_{f_1^i}, \ldots, \bar{u}_{f_{N_u}^i}\right]^T,$$

$$\underline{\sigma}_i = \bar{\sigma}_{\tilde{A}_1^i} \cdots = \bar{\sigma}_{\tilde{A}_{N_u}^i}, \underline{U}_{f_i} \equiv \left[\underline{u}_{f_1^i}, \ldots, \underline{u}_{f_{N_u}^i}\right]^T,$$

and $\underline{\sigma}_i = \underline{\sigma}_{\tilde{A}_1^i}, \cdots = \underline{\sigma}_{\tilde{A}_{N_u}^i}$.

3) Output of the RNT2SFNN is derived

$$o_f = \left(\sum_{i=1}^{N_m} \bar{\phi}_i \bar{\xi}_i(t) + \sum_{i=1}^{N_m} \underline{\phi}_i \underline{\xi}_i(t)\right)/2 \tag{16}$$

where $\bar{\phi}_i = \bar{b}_i^0 + \bar{b}_i^1 u_{f_1}(t) + \cdots + \bar{b}_i^{N_u} u_{f_{N_u}}(t)$ and $\underline{\phi}_i = \underline{b}_i^0 + \underline{b}_i^1 \cdot u_{f_1}(t) + \cdots + \underline{b}_i^{N_u} u_{f_{N_u}}(t)$.

For any continuous function $f(u_f)$, there exists

$$\sup_{u_f \in \mathscr{D}_{u_f}} \left|f(u_f) - \hat{f}(u_f, \phi)\right| \le \varepsilon(u_f), \tag{17}$$

where

$$\phi \equiv \begin{bmatrix} \bar{b}_1^0, \bar{b}_1^1, \ldots, \bar{b}_1^{N_u}, \ldots, \bar{b}_{N_u}^0, \bar{b}_{N_u}^1, \ldots, \bar{b}_{N_u}^{N_u} \\ \underline{b}_1^0, \underline{b}_1^1, \ldots, \underline{b}_1^{N_u}, \ldots, \underline{b}_{N_u}^0, \underline{b}_{N_u}^1, \ldots, \underline{b}_{N_u}^{N_u} \end{bmatrix}^T$$

denotes the weight vector, and $\varepsilon(u_f)$ and $\mathscr{D}_{u_f}$ are the approximation error and the compact set of suitable bounds of$u_f$. Define an optimal parameter $\phi^*$ being equal to $\arg\min_{\phi \in \Omega_\phi}[\sup_{u_f \in \mathscr{D}_{u_f}} |f(u_f) - \hat{f}(u_f, \phi)|]$, where $\Omega_\phi$ is a compact set of $\phi$ and $\hat{f}(u_f, \phi) = o_f$. Let $\tilde{\phi} = \phi - \phi^*$ with $\phi^*$ being an artificial item. Meanwhile, it has $|\varepsilon(u_f)| \le \bar{\varepsilon}$ with $\bar{\varepsilon} > 0$.

A transformation associated with the weight vector for the RNT2SFNN is proposed as

$$\hat{f}\left(u_f,\phi\right)=\phi^T\xi\left(u_f\right)\leq\frac{1}{2B_f^2}\lambda\xi^T\left(u_f\right)\xi\left(u_f\right)+\frac{B_f^2}{2} \quad (18)$$

with $\lambda=\|\phi\|^2$ and $\tilde{\lambda}=\hat{\lambda}-\lambda$, where $\hat{\lambda}$ is the estimation of

$$\lambda,\xi(u_f)\equiv\frac{1}{2}$$

$$\times\begin{bmatrix}\bar{\xi}_1,\bar{\xi}_1u_{f_1},\ldots,\bar{\xi}_1u_{f_{N_u}},\ldots,\bar{\xi}_{N_u},\bar{\xi}_{N_u}u_{f_1},\ldots,\bar{\xi}_{N_u}u_{f_{N_u}}\\ \underline{\xi}_1,\underline{\xi}_1u_{f_1},\ldots,\underline{\xi}_1u_{f_{N_u}},\ldots,\underline{\xi}_{N_u},\underline{\xi}_{N_u}u_{f_1},\ldots,\underline{\xi}_{N_u}u_{f_{N_u}}\end{bmatrix}^T$$

and $B_f>0$.

The self-structuring algorithm of the RNT2SFNN depends on the decreasing rate of tracking error and $\varepsilon$-completeness of fuzzy rules. The training process is summarized: First, compute the tracking error and membership degrees of all MFs; second, ensure$\varepsilon$-completeness; third, compare the threshold of tracking error; and finally, eliminate useless rules based on the membership degrees of the MF.

*Remark 3:* In this article, the RNT2SFNN is proposed to approximate the unknown nonlinear function in a feedforward fuzzy controller and estimate the cost function in an adaptive optimal feedback controller. Through transformation, the quantities of weights significantly reduce to one. It can reduce the computation load and complexity of the controller design.

### B. Speed Function

Explicit design specifications for the well-shaped transient and steady-state behaviors of nonlinear systems are imperative, and not just the tracking errors converge into an unclear residual set. To achieve accelerated convergence, we introduce a rate function in the latter controller design [47], [48]

$$\bar{\rho}\left(t\right)=\begin{cases}\left(\frac{\mathbf{T}}{\mathbf{T}-t}\right)^4\rho\left(t\right), & 0\leq t<\mathbf{T}\\ \infty, & t\geq\mathbf{T}\end{cases} \quad (19)$$

where $0<\mathbf{T}<\infty$ is the time, $\rho(t)$ denotes any nondecreasing and infinite smooth function satisfying $\rho(0)=1$ and $\dot{\rho}(t)\geq 0$. The form of $\rho(t)$ is usually chosen to $1,1+t^2,\mathbf{e}^t$ or $4^t(1+t^2)$.

Then the speed function is constructed as

$$\psi\left(t\right)=1/\left(\left(1-b_\psi\right)\bar{\rho}(t)^{-1}+b_\psi\right) \quad (20)$$

with a design parameter $b_\psi$ satisfying $0<b_\psi<<1$.

With (19), it can be derived from (20) that

$$\psi\left(t\right)=\begin{cases}\frac{\mathbf{T}^4\rho(t)}{(1-b_\psi)(\mathbf{T}-t)^4+b_\psi\mathbf{T}^4\rho(t)}, & 0\leq t<\mathbf{T}\\ 1/b_\psi, & t\geq\mathbf{T}.\end{cases} \quad (21)$$

Note that the speed function $\psi(t)$ is positive and strictly increasing, and has an initial value as $\psi(0)=1$. Furthermore, the choices of $b_\psi$ and $\rho(t)$ directly determine the transient respond and steady-state performance of the controlled system, which explains why the speed function (21) is introduced here. Also, it can be easily verified that ${}^C\mathscr{D}_{0,t}^{\alpha}\psi(t)$ exists and is readily computable from (21). For latter technical development, let $\beta_\psi={}^C\mathscr{D}_{0,t}^{\alpha}\psi(t)/\psi$.

### C. Fuzzy Controller Design

The TD can realize exact estimation for the signal without mathematic expression of the system [30], [49]. In this article, we design a fractional-order TD to obtain the derivative of the virtual control as

$$\begin{cases}{}^C\mathscr{D}_{0,t}^{\alpha}z_{ji}=z_{(j+1)i},{}^C\mathscr{D}_{0,t}^{\alpha}z_{(j+1)i}=-\vartheta_{ji}^2\mathrm{sign}\left(z_{ji}-z_{(r,j)i}\right)\\ \left|z_{ji}-z_{(r,j)i}\right|^{\sigma_{ji}}-\vartheta_{ji}z_{(j+1)i}, \quad j=1,3\end{cases} \quad (22)$$

where $z_{ji}\in\mathbb{R}$ and $z_{(j+1)i}\in\mathbb{R}$ are the states of the TD, $\vartheta_{ji}$ and $\sigma_{ji}$ denote design constants with $\vartheta_{ji}>0$ and $0<\sigma_{ji}<1$, and $z_{(r,j)i}\in\mathbb{R}$ represents the input signal of the TD.

In what follows, the tracking errors $e_{ji}$ and accelerated errors $S_{ji}$ associated with the feedforward fuzzy controller are designed

$$\begin{cases}e_{ji}=x_{ji}-x_{L_j}, & j=1,3\\ e_{ji}=x_{ji}-\alpha_{ji}, & j=2,4\\ S_{ji}=\psi e_{ji}, & j=1,\ldots,4.\end{cases} \quad (23)$$

In (23), $\alpha_{ji}=\alpha_{ji}^a+\alpha_{ji}^*$ is the virtual controller, where $\alpha_i^a$ denotes the virtual control input of the feedforward fuzzy controller and $\alpha_i^*$ is the adaptive optimal feedback control input.

In the framework of the fractional-order backstepping technology, the fuzzy controller design includes four steps.

*Step 1:* The fractional derivative of $S_{1i}$ can be derived as

$${}^C\mathscr{D}_{0,t}^{\alpha}S_{1i}=\psi\left(\beta_\psi e_{1i}+e_{2i}+\alpha_{2i}^a+\alpha_{2i}^*-{}^C\mathscr{D}_{0,t}^{\alpha}x_{L_1}\right). \quad (24)$$

The virtual control is designed as

$$\alpha_{2i}^a=-\left(k_{1i}+\beta_\psi\right)e_{1i}+{}^C\mathscr{D}_{0,t}^{\alpha}x_{L_1} \quad (25)$$

where $k_{1i}$ denotes a design parameter.

Consider the first Lyapunov function candidate as

$$V_{1i}\left(t\right)=\frac{1}{2}S_{1i}^2. \quad (26)$$

Differentiating $V_{1i}(t)$ in (26) yields

$${}^C\mathscr{D}_{0,t}^{\alpha}V_1\left(t\right)=-k_{1i}S_{1i}^2+S_{1i}S_{2i}+S_{1i}\psi\alpha_{2i}^*. \quad (27)$$

*Step 2:* The derivative of $S_{2i}$ can be computed as

$${}^C\mathscr{D}_{0,t}^{\alpha}S_{2i}=\psi$$
$$\times\begin{pmatrix}f_{2i}^*\left(e_{2i}\right)+f_{2i}^a\left(X_i\right)+h_{2i}\left(x_{1i}\left(t-\tau_{1i}\right)\right)+\beta_\psi\\ e_{2i}+\kappa_1\left(x_{1(i-1)}+x_{1(i+1)}\right)+\kappa_2\left(x_{2(i-1)}+x_{2(i+1)}\right)\\ +u_{2i}-{}^C\mathscr{D}_{0,t}^{\alpha}\alpha_{2i}\end{pmatrix} \quad (28)$$

with $f_{2i}^*(e_{2i})\triangleq f_{2i}(X_i)-f_{2i}^a(X_i)$, where $f_{2i}^a(X_i)$ represents an unknown continuous function, $f_{2i}(X_i)=-(\gamma_1+2\kappa_2)x_{2i}-\zeta_1x_{4i}+E_0\cos\omega t$ and $X_i\equiv[x_{1i},x_{2i},x_{3i},x_{4i}]^T$.

For the item $f_{2i}^a(X_i)$, we employ an RNT2SFNN mentioned above to estimate it as

$$f_{2i}^a\left(X_i\right)=\phi_{2i}^T\xi_{2i}\left(X_i\right)+\varepsilon_{2i}\left(X_i\right). \quad (29)$$

Select the Lyapunov–Krasovskii function candidate as

$$V_{2i}(t) = \sum_{j=1}^{2} \frac{1}{1-\bar{\tau}_{\max}} \mathbf{e}^{-\kappa_i(t-\tau_{1i})} \times \int_{t-\tau_{1i}}^{t} \mathbf{e}^{\kappa_i\theta} S_{ji}^2(\theta)\, q_{2j}^2(x_{1i}, x_{2i})\, d\theta + V_{1i}(t) + \frac{1}{2}S_{2i}^2 + \frac{1}{2\mu_{2i}}\tilde{\lambda}_{2i}^2 \tag{30}$$

where $\mu_{2i}$ and $\kappa_i$ denote the constants.

Taking the derivative of $V_{2i}(t)$ with respect to time obtains

$$\begin{aligned}
{}^{C}\mathscr{D}_{0,t}^{\alpha} V_{2i}(t) \le{}& -\kappa_i \mathbf{e}^{-\kappa_i(t-\tau_{1i})} \sum_{j=1}^{2} \\
&\times \int_{t-\tau_{1i}}^{t} \mathbf{e}^{\kappa_i\theta} S_{ji}^2(\theta)\, q_{2j}^2(x_{1i}, x_{2i})\, d\theta + \frac{\mathbf{e}^{\kappa_i\tau_{1i}}}{1-\bar{\tau}_{\max}} \\
&\times \sum_{j=1}^{2} S_{ji}^2(t)\, q_{2j}^2(x_{1i}(t), x_{2i}(t)) - k_{1i}S_{1i}^2 + S_{1i}\psi\alpha_{2i}^* + \psi S_{2i} \\
&\cdot h_{2i}(x_{1i}(t-\tau_{1i})) \\
&- \sum_{j=1}^{2} S_{ji}^2(t-\tau_{1i})\, q_{2j}^2(x_{1i}(t-\tau_{1i}), x_{2i}(t-\tau_{1i})) \\
&+ S_{2i}\psi \begin{pmatrix} \beta_\psi e_{2i} + f_{2i}^*(e_{2i}) + \kappa_1\left(x_{1(i-1)} + x_{1(i+1)}\right) \\ +e_{1i} + u_{2i}^a + u_{2i}^* + \kappa_2 \\ \left(x_{2(i-1)} + x_{2(i+1)}\right) - {}^{C}\mathscr{D}_{0,t}^{\alpha}\alpha_{2i} \\ +\frac{1}{2B_{2i}^2} S_{2i}\psi\hat{\lambda}_{2i}\xi_{2i}^T(X_i)\,\xi_{2i}(X_i) \end{pmatrix} \\
&+ \frac{\tilde{\lambda}_{2i}}{\mu_{2i}}\left[{}^{C}\mathscr{D}_{0,t}^{\alpha}\tilde{\lambda}_{2i} - \frac{\mu_{2i}}{2B_{2i}^2} S_{2i}^2\psi^2\xi_{2i}^T(X_i)\,\xi_{2i}(X_i)\right] \\
&+ S_{2i}\psi\xi_{2i}(X_i) + \frac{B_{2i}^2}{2}.
\end{aligned} \tag{31}$$

Note that

$$S_{2i}\psi\varepsilon_{2i}(X_i) \le \frac{1}{2}S_{2i}^2\psi^2 + \frac{1}{2}\bar{\varepsilon}_{2i}^2 \tag{32}$$

$$\begin{aligned}
&\psi S_{2i} h_{2i}(x_{1i}(t-\tau_{1i})) \\
&\le \psi S_{2i} \sum_{j=1}^{2} |S_{ji}(t-\tau_{1i})| \cdot \\
&\quad q_{2j}(x_{1i}(t-\tau_{1i}), x_{2i}(t-\tau_{1i})) \\
&\le \frac{\psi^2 S_{2i}^2}{2} + \sum_{j=1}^{2} \left|S_{ji}^2(t-\tau_{1i})\right| q_{2j}^2(x_{1i}(t-\tau_{1i}), x_{2i}(t-\tau_{1i})).
\end{aligned} \tag{33}$$

It is difficult to directly calculate ${}^{C}\mathscr{D}_{0,t}^{\alpha}\alpha_{2i}$. So we employ a fractional-order TD to approximate it here. Substituting (32) and (33) into (31) yields

$$\begin{aligned}
{}^{C}\mathscr{D}_{0,t}^{\alpha} V_{2i}(t) \le{}& -\kappa_i \mathbf{e}^{-\kappa_i(t-\tau_{1i})} \sum_{j=1}^{2} \\
&\times \int_{t-\tau_{1i}}^{t} \mathbf{e}^{\kappa_i\theta} S_{ji}^2(\theta)\, q_{2j}^2(x_{1i}, x_{2i})\, d\theta + S_{2i} \\
&\cdot \psi \begin{pmatrix} \beta_\psi e_{2i} + f_{2i}^*(e_{2i}) + \kappa_1\left(x_{1(i-1)} + x_{1(i+1)}\right) \\ +e_{1i} + u_{2i}^a + u_{2i}^* + \kappa_2 \\ \left(x_{2(i-1)} + x_{2(i+1)}\right) - z_{2i} \\ +\frac{1}{2B_{2i}^2} S_{2i}\psi\hat{\lambda}_{2i}\xi_{2i}^T(X_i)\,\xi_{2i}(X_i) + S_{2i}\psi \end{pmatrix} \\
&+ \frac{\tilde{\lambda}_{2i}}{\mu_{2i}}\left[{}^{C}\mathscr{D}_{0,t}^{\alpha}\hat{\lambda}_{2i} - \frac{\mu_{2i}}{2B_{2i}^2} S_{2i}^2\psi^2\xi_{2i}^T(X_i)\,\xi_{2i}(X_i)\right] \\
&- k_{1i}S_{1i}^2 + S_{1i}\psi\alpha_{2i}^* + \frac{1}{2}\bar{\varepsilon}_{2i}^2 + \frac{B_{2i}^2}{2}.
\end{aligned} \tag{34}$$

*Remark 4:* For Caputo fractional derivative, it has ${}^{C}\mathscr{D}_{0,t}^{\alpha}\tilde{\lambda}_{ji} = {}^{C}\mathscr{D}_{0,t}^{\alpha}\hat{\lambda}_{ji}$ with ${}^{C}\mathscr{D}_{0,t}^{\alpha}\lambda_{ji} = 0, j = 2, 4$. If we choose the RL fractional derivative to continue controller design, ${}^{\mathrm{RL}}\mathscr{D}_{0,t}^{\alpha}\lambda_{ji} = \lambda_{ji}t^{-\alpha}/\Gamma(1-\alpha)$, $j = 2, 4$ exist. There is a conversion relationship between two derivatives such that ${}^{\mathrm{RL}}\mathscr{D}_{0,t}^{\alpha}\tilde{\lambda}_{ji} = {}^{C}\mathscr{D}_{0,t}^{\alpha}\tilde{\lambda}_{ji} + \tilde{\lambda}_{ji}(0)t^{-\alpha}/\Gamma(1-\alpha)$. So the proposed scheme exhibits wider applications.

The control input with an adaptive law is designed as

$$\begin{aligned}
u_{2i}^a = {}& -(k_{2i} + \beta_\psi)\, e_{2i} - \frac{1}{2B_{2i}^2} S_{2i}\psi\hat{\lambda}_{2i}\xi_{2i}^T(X_i)\,\xi_{2i}(X_i) - e_{1i} \\
&+ z_{2i} - S_{2i}\psi - \kappa_1\left(x_{1(i-1)} + x_{1(i+1)}\right) \\
&- \kappa_2\left(x_{2(i-1)} + x_{2(i+1)}\right)
\end{aligned} \tag{35}$$

$${}^{C}\mathscr{D}_{0,t}^{\alpha}\hat{\lambda}_{2i} = \mu_{2i}\left[\frac{1}{2B_{2i}^2} S_{2i}^2\psi^2\xi_{2i}^T(X_i)\,\xi_{2i}(X_i) - g_{2i}\hat{\lambda}_{2i}\right] \tag{36}$$

with $\mu_{2i}$, $g_{2i}$, and $k_{2i}$being positive constants.

With (35) and (36), (34) is rewritten as

$$\begin{aligned}
{}^{C}\mathrm{D}_{0,t}^{\alpha} V_{2i}(t) \le{}& -\kappa_i \mathbf{e}^{-\kappa_i(t-\tau_{1i})} \sum_{j=1}^{2} \\
&\times \int_{t-\tau_{1i}}^{t} \mathbf{e}^{\kappa_i\theta} S_{ji}^2(\theta)\, q_{2j}^2(x_{1i}, x_{2i})\, d\theta \\
&+ S_{2i}\psi\left(f_{2i}^*(e_{2i}) + u_{2i}^*\right) + S_{1i}\psi\alpha_{2i}^* \\
&- \sum_{j=1}^{2} k_{1i}S_{1i}^2 - g_{2i}\tilde{\lambda}_{2i}\hat{\lambda}_{2i} + \frac{B_{2i}^2}{2} + \frac{1}{2}\bar{\varepsilon}_{2i}^2.
\end{aligned} \tag{37}$$

*Step 3:* Choose the Lyapunov function candidate as

$$V_{3i}(t) = V_{2i}(t) + \frac{1}{2}S_{3i}^2. \tag{38}$$

Taking the derivative of $V_{3i}(t)$ yields

$$\begin{aligned}
{}^{C}\mathscr{D}_{0,t}^{\alpha} V_{3i}(t) \le{}& -\kappa_i \mathbf{e}^{-\kappa_i(t-\tau_{1i})} \sum_{j=1}^{2} \\
&\times \int_{t-\tau_{1i}}^{t} \mathbf{e}^{\kappa_i\theta} S_{ji}^2(\theta)\, q_{2j}^2(x_{1i}, x_{2i})\, d\theta
\end{aligned}$$

$$+ S_{2i}\psi\left(f_{2i}^{*}\left(e_{2i}\right)+u_{2i}^{*}\right)+S_{1i}\psi\alpha_{2i}^{*}$$
$$-\sum_{j=1}^{2}k_{ji}S_{ji}^{2}-g_{2i}\tilde{\lambda}_{2i}\hat{\lambda}_{2i}+\frac{B_{2i}^{2}}{2}$$
$$+\frac{1}{2}\bar{\varepsilon}_{2i}^{2}+S_{3i}\psi\left(\beta_{\psi}e_{3i}+e_{4i}+\alpha_{4i}^{a}+\alpha_{4i}^{*}-{}^{C}\mathscr{D}_{0,t}^{\alpha}x_{L_3}\right). \tag{39}$$

Then the virtual control is chosen as

$$\alpha_{4i}^{a}=-\left(k_{3i}+\beta_{\psi}\right)e_{3i}+{}^{C}\mathscr{D}_{0,t}^{\alpha}x_{L_3} \tag{40}$$

where $k_{3i}$ denotes the design parameter.

Whereafter, substituting (40) into (39) yields

$${}^{C}\mathscr{D}_{0,t}^{\alpha}V_{3i}\left(t\right)\leq-\kappa_i\mathbf{e}^{-\kappa_i\left(t-\tau_{1i}\right)}\sum_{j=1}^{2}$$
$$\times\int_{t-\tau_{1i}}^{t}\mathbf{e}^{\kappa_i\theta}S_{ji}^{2}\left(\theta\right)q_{2j}^{2}\left(x_{1i},x_{2i}\right)d\theta$$
$$+S_{2i}\psi\left(f_{2i}^{*}\left(e_{2i}\right)+u_{2i}^{*}\right)+\sum_{j=1,3}S_{ji}\psi\alpha_{(j+1)i}^{*}$$
$$-\sum_{j=1}^{3}k_{ji}S_{ji}^{2}+S_{3i}S_{4i}-g_{2i}\tilde{\lambda}_{2i}\hat{\lambda}_{2i}+\frac{B_{2i}^{2}}{2}+\frac{1}{2}\bar{\varepsilon}_{2i}^{2}. \tag{41}$$

*Step 4:* Consider the Lyapunov–Krasovskii function candidate

$$V_{4i}(t)=\sum_{j=3}^{4}\frac{1}{1-\bar{\tau}_{\max}}\mathbf{e}^{-\kappa_i\left(t-\tau_{3i}\right)}\int_{t-\tau_{3i}}^{t}$$
$$\times\mathbf{e}^{\kappa_i\theta}S_{ji}^{2}(\theta)q_{4j}^{2}(x_{3i},x_{4i})d\theta+V_{3i}(t)+\frac{1}{2}S_{4i}^{2}+\frac{1}{2\mu_{4i}}\tilde{\lambda}_{4i}^{2}$$

with $\mu_{4i}$ being a positive constant.

Taking the fractional derivative of $S_{4i}$, we get

$${}^{C}\mathscr{D}_{0,t}^{\alpha}S_{4i}$$
$$=\psi\begin{pmatrix}f_{4i}^{*}\left(e_{4i}\right)+f_{4i}^{a}\left(X_i\right)+h_{4i}\left(x_{3i}\left(t-\tau_{3i}\right)\right)+u_{4i}\\+\beta_{\psi}e_{4i}-{}^{C}\mathscr{D}_{0,t}^{\alpha}\alpha_{4i}\end{pmatrix} \tag{42}$$

with $f_{4i}^{*}(e_{4i})\triangleq f_{4i}(X_i)-f_{4i}^{a}(X_i)$, where $f_{4i}^{a}(X_i)$ represents a continuous function and $f_{4i}(X_i)=-\gamma_2x_{4i}+\zeta_2x_{2i}$.

For unknown nonlinear function $f_{4i}^{a}(X_i)$, we use an RNT2SFNN mentioned above to approximate it with high precision such that $f_{4i}^{a}(X_i)=\phi_{4i}^{T}\xi_{4i}(X_i)+\varepsilon_{4i}(X_i)$. Similarly, to avoid complex calculation for the item ${}^{C}\mathscr{D}_{0,t}^{\alpha}\alpha_{4i}$, we employ the fractional-order TD to approximate it. That is, ${}^{C}\mathscr{D}_{0,t}^{\alpha}\alpha_{4i}=z_{4i}$.

Invoking Assumption 2 and Young's inequality, we have

$$\psi S_{4i}h_{4i}\left(x_{3i}\left(t-\tau_{3i}\right)\right)\leq\sum_{j=1}^{2}\left|S_{ji}^{2}\left(t-\tau_{3i}\right)\right|\cdot$$
$$q_{4j}^{2}\left(x_{3i}\left(t-\tau_{3i}\right),x_{4i}\left(t-\tau_{3i}\right)\right)+\frac{\psi^{2}S_{4i}^{2}}{2} \tag{43}$$

$$S_{4i}\psi\varepsilon_{4i}\left(X_i\right)\leq\frac{1}{2}S_{4i}^{2}\psi^{2}+\frac{1}{2}\bar{\varepsilon}_{4i}^{2}. \tag{44}$$

By a series of transformations, the derivative of $V_{4i}(t)$ can be deduced from (42) to (44) as

$${}^{C}\mathrm{D}_{0,t}^{\alpha}V_{4i}\left(t\right)\leq-\sum_{J=1,3}\kappa_i\mathbf{e}^{-\kappa_i\left(t-\tau_{Ji}\right)}$$
$$\times\sum_{j=J}^{J+1}\int_{t-\tau_{Ji}}^{t}\mathbf{e}^{\kappa_i\theta}S_{ji}^{2}\left(\theta\right)q_{(J+1)j}^{2}\left(x_{Ji},x_{(J+1)i}\right)d\theta$$
$$+S_{4i}\psi\begin{pmatrix}\beta_{\psi}e_{4i}+f_{4i}^{*}\left(e_{4i}\right)+\frac{1}{2B_{4i}^{2}}S_{4i}\psi\hat{\lambda}_{4i}\xi_{4i}^{T}\left(X_i\right)\xi_{4i}\left(X_i\right)\\+S_{4i}\psi+e_{3i}+u_{4i}^{a}+u_{4i}^{*}-z_{4i}\end{pmatrix}$$
$$+\frac{\tilde{\lambda}_{4i}}{\mu_{4i}}\left[{}^{C}\mathrm{D}_{0,t}^{\alpha}\hat{\lambda}_{4i}-\frac{\mu_{4i}}{2B_{4i}^{2}}S_{4i}^{2}\psi^{2}\xi_{4i}^{T}\left(X_i\right)\xi_{4i}\left(X_i\right)\right]$$
$$-\sum_{j=1}^{3}k_{ji}S_{ji}^{2}+\sum_{j=2,4}\frac{B_{ji}^{2}}{2}+\sum_{j=1,3}S_{ji}\psi\alpha_{(j+1)i}^{*}$$
$$+S_{2i}\psi\left(f_{2i}^{*}\left(e_{2i}\right)+u_{2i}^{*}\right)+\sum_{j=2,4}\frac{1}{2}\bar{\varepsilon}_{2i}^{2}-g_{2i}\tilde{\lambda}_{2i}\hat{\lambda}_{2i}. \tag{45}$$

Choose the control input as

$$u_{4i}^{a}=-\left(k_{4i}+\beta_{\psi}\right)e_{4i}$$
$$-\frac{1}{2B_{4i}^{2}}S_{4i}\psi\hat{\lambda}_{4i}\xi_{4i}^{T}\left(X_i\right)\xi_{4i}\left(X_i\right)-S_{4i}\psi-e_{3i}+z_{4i} \tag{46}$$

where $k_{4i}$ is a positive constant.

Then a fractional-order adaptation law is selected as

$${}^{C}\mathscr{D}_{0,t}^{\alpha}\hat{\lambda}_{4i}=\mu_{4i}\left(\frac{1}{2B_{4i}^{2}}S_{4i}^{2}\psi^{2}\xi_{4i}^{T}\left(X_i\right)\xi_{4i}\left(X_i\right)-g_{4i}\hat{\lambda}_{4i}\right) \tag{47}$$

with $\mu_{4i}$ and $g_{4i}$ being positive constants.

According to (46) and (47), (45) can further be deduced as

$${}^{C}\mathscr{D}_{0,t}^{\alpha}V_{4i}\left(t\right)\leq-\sum_{J=1,3}\kappa_i\mathbf{e}^{-\kappa_i\left(t-\tau_{Ji}\right)}$$
$$\times\sum_{j=J}^{J+1}\int_{t-\tau_{Ji}}^{t}\mathbf{e}^{\kappa_i\theta}S_{ji}^{2}\left(\theta\right)q_{(J+1)j}^{2}\left(x_{Ji},x_{(J+1)i}\right)d\theta$$
$$+\sum_{j=2,4}S_{ji}\psi\left(f_{ji}^{*}\left(e_{ji}\right)+u_{ji}^{*}\right)-\sum_{j=1}^{4}k_{ji}S_{ji}^{2}+\sum_{j=2,4}\frac{B_{ji}^{2}}{2}$$
$$+\sum_{j=1,3}S_{ji}\psi\alpha_{(j+1)i}^{*}$$
$$+\sum_{j=2,4}\frac{1}{2}\bar{\varepsilon}_{ji}^{2}-\frac{3}{2}\sum_{j=2,4}g_{ji}\tilde{\lambda}_{ji}^{2}-\frac{1}{2}\sum_{j=2,4}g_{ji}\lambda_{ji}^{2}. \tag{48}$$

We define two vectors such that $\mathbf{S}_i\equiv[S_{1i},S_{2i},S_{3i},S_{4i}]^{T}$ and $U_i^{*}\equiv[\alpha_{2i}^{*},u_{2i}^{*},\alpha_{4i}^{*},u_{4i}^{*}]^{T}$. Then (48) can be rewritten as

$${}^{C}\mathscr{D}_{0,t}^{\alpha}V_{4i}\left(t\right)\leq-\sum_{J=1,3}\kappa_i\mathbf{e}^{-\kappa_i\left(t-\tau_{Ji}\right)}$$
$$\times\sum_{j=J}^{J+1}\int_{t-\tau_{Ji}}^{t}\mathbf{e}^{\kappa_i\theta}S_{ji}^{2}\left(\theta\right)q_{(J+1)j}^{2}\left(x_{Ji},x_{(J+1)i}\right)d\theta$$

$$-\sum_{j=1}^{4} k_{ji} S_{ji}^2 - \frac{3}{2}\sum_{j=2,4} g_{ji}\tilde{\lambda}_{ji}^2 + \psi \mathbf{S}_i^T \left\{ \begin{bmatrix} 0 \\ f_{2i}^*(e_{2i}) \\ 0 \\ f_{4i}^*(e_{4i}) \end{bmatrix} + \mathbf{I}_{4\times 4} U_i^* \right\} + \Xi_i \tag{49}$$

where $\Xi_i = \sum_{j=2,4} \frac{B_{ji}^2}{2} + \sum_{j=2,4} \frac{1}{2}\bar{\varepsilon}_{ji}^2 - \frac{1}{2}\sum_{j=2,4} g_{ji}\lambda_{ji}^2$.

*Remark 5:* It is worth pointing out that the whole controller $U_i$ is composed of two components: a feedforward fuzzy controller $U_i^a \equiv [\alpha_{2i}^a, u_{2i}^a, \alpha_{4i}^a, u_{4i}^a]^T$ and an optimal feedback controller $U_i^*$. The latter depends on the former, and they are not parallel. $U_i^a$ does not guarantee the stability of the whole closed-loop coupled electromechanical transducers when $U_i^*$ equals zero. Furthermore, the proposed feedforward fuzzy controller cannot involve any sort of optimality. In view of this, we should develop an optimal feedback controller to realize the purposes such that the cost function is smallest and the closed-loop system is stable.

*Remark 6:* The problem of "explosion of complexity" associated with the traditional fractional-order backstepping is inevitable along with the order increase [26], [50]. We employ a TD to tackle this problem. Besides, we design a speed function to obtain a desirable convergence rate as fast as exponential or even faster.

Then, the fractional-order nonlinear system for the optimal feedback controller is given as

$${}^{C}\mathrm{D}_{0,t}^{\alpha}\mathbf{S}_i = [0 f_{2i}^*(e_{2i})\, 0 f_{4i}^*(e_{4i})]^T + \mathbf{I}_{4\times 4} U_i^*. \tag{50}$$

## IV. Adaptive Optimal Feedback Controller Design

In this section, an adaptive optimal feedback control scheme is developed to stabilize the affine system (50). Most fractional-order controllers do not consider optimality. It is seen that the optimal control further improves the performance.

We rewrite (50) as

$${}^{C}\mathrm{D}_{0,t}^{\alpha}\mathbf{S}_i = \mathrm{H_i}(\mathbf{S}_i) + G_i U_i^* \tag{51}$$

where $\mathrm{H_i}(\mathbf{S}_i) \equiv [0 f_{2i}^*(e_{2i}) 0 f_{4i}^*(e_{4i})]^T$ and $G_i$ is a fourth-rank identity matrix.

Define the Hamiltonian function

$$\bar{\boldsymbol{H}}_i^o(\mathbf{S}_i, U_i^*, \nabla J_i) = Q_i(\mathbf{S}_i) + {U_i^*}^T R_i U_i^* + (\nabla J_i)^T (\mathrm{H_i}(\mathbf{S}_i) + G_i U_i^*) \tag{52}$$

with $\nabla J_i$ denoting the gradient of $J_i(\mathbf{S}_i)$.

The optimal cost function $J_i^*(\mathbf{S}_i)$ in (12) satisfies the HJB equation as $0 = \min_{U_i^* \in \psi(\Omega)} \bar{\boldsymbol{H}}_i^o(\mathbf{S}_i, U_i^*, \nabla J_i^*)$. We assume this equation exists and is unique. Then an adaptive optimal feedback control input $U_i^*$ is derived as

$$U_i^* = -\frac{1}{2} R_i^{-1} G_i^T \nabla J_i^*(\mathbf{S}_i) \tag{53}$$

where $\nabla J_i^*(\mathbf{S}_i)$ denotes the gradient of $J_i^*(\mathbf{S}_i)$.

**Algorithm 1:** PI Algorithm for Optimal Control Problem.

a) Start with stabilizing initial policy $U_i^0$ to ensure the convergence of the algorithm.
b) Given $U_i^{\mathbf{k}}$, solve for the value $J_i^{\mathbf{k}}(\mathbf{S}_i)$ using $0 = Q_i(\mathbf{S}_i) + (U_i^{\mathbf{k}})^T R U_i^{\mathbf{k}} + (\nabla J_i^{\mathbf{k}}(\mathbf{S}_i))^T (\mathrm{H_i}(\mathbf{S}_i) + G_i U_i^{\mathbf{k}})$, $J_i^{\mathbf{k}}(0) = 0$.
c) Update control policy using $U_i^{\mathbf{k}+1} = \underset{U_i \in \Psi(X_i)}{\operatorname{argmin}} \bar{\boldsymbol{H}}_i^o(\mathbf{S}_i, U_i, \nabla J_i^{\mathbf{k}}(\mathbf{S}_i))$ which explicitly is $U_i^{\mathbf{k}+1} = -\frac{1}{2} R_i^{-1} G_i^T \nabla J_i^{\mathbf{k}}(\mathbf{S}_i)$.

Substituting (53) into (52) can obtain the formulation of the HJB equation for $J_i^*$

$$Q_i(\mathbf{S}_i) + (\nabla J_i^*(\mathbf{S}_i))^T \mathrm{H_i}(\mathbf{S}_i) - \frac{1}{4}(\nabla J_i^*(\mathbf{S}_i))^T G_i R_i^{-1} G_i^T \nabla J_i^*(\mathbf{S}_i) = 0\, J_i^*(0) = 0. \tag{54}$$

*Lemma 2:* Given the controlled system (51) with cost function (12) and optimal control input (53), there exists a continuous differentiable and unbound Lyapunov function $J_{io}(\mathbf{S}_i)$ satisfying ${}^{C}\mathscr{D}_{0,t}^{\alpha} J_{io}(\mathbf{S}_i) = \nabla J_{io}(\mathbf{S}_i)(\mathrm{H_i}(\mathbf{S}_i) + G_i U_i^*) < 0$, where $\nabla J_{io}(\mathbf{S}_i)$ denotes the partial derivative of $J_{io}(\mathbf{S}_i)$. Introduce a positive definite function $\Lambda_i(\mathbf{S}_i)$satisfying $\lim_{\mathbf{S}_i \to 0} \Lambda_i(\mathbf{S}_i) = 0$ and $\lim_{\mathbf{S}_i \to \infty} \Lambda_i(\mathbf{S}_i) = \infty$ as well as

$$\nabla J_i^T(\mathbf{S}_i) \Lambda_i(\mathbf{S}_i) \nabla J_{io}(\mathbf{S}_i) = Q_i(\mathbf{S}_i) + {U_i^*}^T R_i U_i^*. \tag{55}$$

Then the following inequation can be obtained:

$$\nabla J_i(\mathbf{S}_i)(\mathrm{H_i}(\mathbf{S}_i) + G_i U_i^*) < -\nabla J_{io}^T(\mathbf{S}_i) \Lambda_i(\mathbf{S}_i) \nabla J_{io}(\mathbf{S}_i). \tag{56}$$

The PI algorithm [34], [40], which consists of the policy improvement based on (53) and the policy evaluation upon the Bellman equation, is taken as an efficient solution to solve the HJB (54). Unfortunately, unknown system dynamics such as $\mathrm{H_i}(\mathbf{S}_i)$ result in the difficulty of solving the HJB equation. To cope with this issue concerned, we employ the RNT2SFNN to approximate the critic value and the actor control functions and use the PI algorithm tuning the RNT2SFNN.

The Algorithm 1 can converge to the optimal control polity $U_i^*$ with corresponding cost function $J_i^*(\mathbf{S}_i)$.

Based on the value function approximation, the cost function $J_i(\mathbf{S}_i)$ as well as its gradient can be approximated in Sobolev space such that

$$J_i(\mathbf{S}_i) = \phi_{\mathrm{in}}^T \xi_{\mathrm{in}}(\mathbf{S}_i) + \varepsilon_{\mathrm{in}}(\mathbf{S}_i). \tag{57}$$

The gradient of (57) is written as

$$\nabla J_i(\mathbf{S}_i) = \nabla \xi_{\mathrm{in}}^T(\mathbf{S}_i) \phi_{\mathrm{in}} + \nabla \varepsilon_{\mathrm{in}}(\mathbf{S}_i). \tag{58}$$

Substituting (58) into (53), it can be obtained that

$$U_i^* = -\frac{1}{2} R_i^{-1} G_i^T \left(\nabla \xi_{\mathrm{in}}^T(\mathbf{S}_i) \phi_{\mathrm{in}} + \nabla \varepsilon_{\mathrm{in}}(\mathbf{S}_i)\right). \tag{59}$$

The HJB equation is further derived as

$$\bar{\boldsymbol{H}}_i^o(\mathbf{S}_i, \phi_{\mathrm{in}}) = Q_i(\mathbf{S}_i) + \phi_{\mathrm{in}}^T \nabla \xi_{\mathrm{in}}(\mathbf{S}_i) \mathrm{H_i}(\mathbf{S}_i) - \frac{1}{4}\phi_{\mathrm{in}}^T \nabla \xi_{\mathrm{in}}(\mathbf{S}_i) \cdot \hbar_i \nabla \xi_{\mathrm{in}}^T(\mathbf{S}_i) \phi_{\mathrm{in}} + e_{i_{\mathrm{HJB}}}, \tag{60}$$

where $\hbar_i = G_i R_i^{-1} G_i^T$, and the residual error $e_{i_{\mathrm{HJB}}}$ is defined as $e_{i_{\mathrm{HJB}}} = \nabla\varepsilon_{\mathrm{in}}^T(\mathbf{S}_i)(G_i U_i^* + \mathrm{H_i}(\mathbf{S}_i)) + \frac{1}{4}\nabla\varepsilon_{\mathrm{in}}^T(\mathbf{S}_i)\hbar_i\nabla\varepsilon_{\mathrm{in}}(\mathbf{S}_i)$.

According to [38], the optimal closed-loop dynamical system is bounded such that

$$\|G_i U_i^* + \mathrm{H_i}\left(\mathbf{S}_i\right)\| \le c_{io}\sqrt{\|\mathbf{S}_i\|}, \tag{61}$$

where $c_{io}$ represents a positive constant.

Because the weights for the output of the actor/critic RNT2SFNN are unknown, we use the current known weights to replace them such that

$$\hat{J}_i\left(\mathbf{S}_i\right) = \hat{\phi}_{\mathrm{in}}^T \xi_{\mathrm{in}}\left(\mathbf{S}_i\right) \tag{62}$$

where $\hat{\phi}_{\mathrm{in}}$ denotes the estimation of $\phi_{\mathrm{in}}$. Besides, the weight error $\tilde{\phi}_{\mathrm{in}}$ equals $\phi_{\mathrm{in}} - \hat{\phi}_{\mathrm{in}}$.

The optimal feedback controller is designed in the structured form

$$\hat{U}_i = -\frac{1}{2} R_i^{-1} G_i^T \nabla\xi_{\mathrm{in}}^T\left(\mathbf{S}_i\right)\hat{\phi}_{\mathrm{in}}. \tag{63}$$

Then the HJB equation becomes

$$\begin{aligned}\bar{\boldsymbol{H}}_i^o\left(\mathbf{S}_i, \hat{\phi}_{\mathrm{in}}, \hat{U}_i\right) &= Q_i\left(\mathbf{S}_i\right) + \hat{\phi}_{\mathrm{in}}^T \nabla\xi_{\mathrm{in}}\left(\mathbf{S}_i\right)\mathrm{H_i}\left(\mathbf{S}_i\right) \\ &\quad - \frac{1}{4}\hat{\phi}_{\mathrm{in}}^T \bar{D}_i \hat{\phi} l_{\mathrm{in}} \triangleq e_{\mathrm{in}}\end{aligned} \tag{64}$$

where

$$\bar{D}_i = \nabla\xi_{\mathrm{in}}\left(\mathbf{S}_i\right) G_i R_i^{-1} G_i^T \nabla\xi_{\mathrm{in}}^T\left(\mathbf{S}_i\right).$$

Recalling the HJB equation (54), it is desired to choose $\hat{\phi}_{\mathrm{in}}$ to minimize the squared residual error

$$V_{\mathrm{in}}\left(t\right) = \frac{1}{2} e_{\mathrm{in}}^T e_{\mathrm{in}}. \tag{65}$$

Obviously, only turning $e_{\mathrm{in}}$ does not guarantee the stability of the controlled system (51). Therefore, an adaptive law for the actor/critic RNT2SFNN is designed as

$$\begin{aligned}{}^C\mathrm{D}_{0,t}^{\alpha}\hat{\phi}_{\mathrm{in}} &= a_{\mathrm{in}}\left(\frac{\varpi_{\mathrm{in}}}{4\underline{m}_{\mathrm{in}}^2}\hat{\phi}_{\mathrm{in}}^T\bar{D}_i\hat{\phi}_{\mathrm{in}} - F_{in_2}\hat{\phi}_{\mathrm{in}} + F_{\mathrm{in}_1}\varphi_{\mathrm{in}}^T\hat{\phi}_{\mathrm{in}}\right) \\ &\quad - \frac{a_{\mathrm{in}}}{\underline{m}_{\mathrm{in}}^2}\varpi_{\mathrm{in}}e_{\mathrm{in}} + \frac{a_{\mathrm{in}}}{2}\sum\left(\mathbf{S}_i, \hat{U}_i\right)\nabla\xi_{\mathrm{in}}\hbar_i\nabla J_{io}\left(\mathbf{S}_i\right)\end{aligned} \tag{66}$$

where $\varpi_{\mathrm{in}} = \nabla\xi_{\mathrm{in}}(\mathrm{H_i}(\mathbf{S}_i) + G_i\hat{U}_i)$, $\underline{m}_{\mathrm{in}} = 1 + \nabla\xi_{\mathrm{in}}^T\nabla\xi_{\mathrm{in}}$, $\varphi_{\mathrm{in}} = \varpi_{\mathrm{in}}/\underline{m}_{\mathrm{in}}$, $F_{\mathrm{in}_1}$, and $F_{\mathrm{in}_2}$ are the tuning parameters, $a_{\mathrm{in}}$ denotes a positive tuning parameter which directly determines the speed of learning, and $\sum(\mathbf{S}_i, \hat{U}_i)$ is an operator defined as

$$\sum\left(\mathbf{S}_i, \hat{U}_i\right) = \begin{cases} 0, & \text{if } {}^C\mathrm{D}_{0,t}^{\alpha}\nabla J_{io}\left(\mathbf{S}_i\right) < 0 \\ 1, & \text{else.}\end{cases} \tag{67}$$

*Remark 7:* The adaptive law (66) includes three terms in which the first one is used for stability analysis, the second term seeks to minimize $e_{\mathrm{in}}$, and the last item guarantees the boundness of system states. $Q_i(\mathbf{S}_i) > 0$ is sufficient but not necessary here. In addition, (63) and (66) depend on $\mathrm{H_i}(\mathbf{S}_i)$ and $G_i$.

*Remark 8:* The initial weight vector of adaptive law for the actor/critic RNT2SFNN is chosen to be a zero vector due to adding the third item of (66). $F_{\mathrm{in}_1}$ and $F_{\mathrm{in}_2}$ must be chosen to ensure the positive definition of the matrix $\bar{\mathrm{G}}_s$, where unnumberd eq. shown at the bottom of this page, with $\bar{\beta}_i^*$ satisfying $e_i^T\bar{\beta}_i^* e_i < \bar{\gamma}_i^*(e_i)$ and $\bar{\gamma}_i^*(e_i) > 0$.

## V. Stability Analysis

*Theorem 1:* Considering the three coupled fractional-order electromechanical transducers (6) with unknown nonlinear functions, chaotic oscillations, and time-varying time delays under Assumptions 1–3, design the feedforward fuzzy control inputs be (25), (35), (40), and (46) with adaptive laws as (36) and (47). If the adaptive optimal feedback control input is chosen as (63) with an updated law (66) for the actor/critic RNT2SFNN, the following conclusions hold.

1) All signals including the system states and adaptive parameters are bounded.
2) The chaos suppression, synchronization, and accelerated convergence and time delay are well addressed.
3) The cost function is minimized.

*Proof:* Consider the whole Lyapunov function candidate as

$$V\left(t\right) = \frac{1}{2a_{\mathrm{in}}}\tilde{\phi}_{\mathrm{in}}^T\left(t\right)\tilde{\phi}_{\mathrm{in}}\left(t\right) + J_{io}\left(\mathbf{S}_i\right) + V_4\left(t\right). \tag{68}$$

By taking the derivative for $V(t)$, it has

$$\begin{aligned}&{}^C\mathscr{D}_{0,t}^{\alpha}V\left(t\right) = \tilde{\phi}_{\mathrm{in}}^T \\ &\times\begin{bmatrix}\frac{\varphi_{\mathrm{in}}}{\underline{m}_{\mathrm{in}}}\left(\frac{1}{2}\phi_{\mathrm{in}}^T\bar{D}_i\tilde{\phi}_{\mathrm{in}} - \frac{1}{4}\phi_{\mathrm{in}}^T\bar{D}_i\phi_{\mathrm{in}}\right) + F_{\mathrm{in}_2}\left(\phi_{\mathrm{in}} - \tilde{\phi}_{\mathrm{in}}\right) \\ -F_{\mathrm{in}_1}\varphi_{\mathrm{in}}^T\left(\phi_{\mathrm{in}} - \tilde{\phi}_{\mathrm{in}}\right) + \frac{\varphi_{\mathrm{in}}}{\underline{m}_{\mathrm{in}}}\left(-\tilde{\phi}_{\mathrm{in}}^T\varpi_{\mathrm{in}} - e_{i_{\mathrm{HJB}}}\right)\end{bmatrix} \\ &- \frac{1}{2}\tilde{\phi}_{\mathrm{in}}^T\sum\left(\mathbf{S}_i, \hat{U}_i\right)\nabla\xi_{\mathrm{in}}\hbar_i\nabla J_{io}\left(\mathbf{S}_i\right) + \nabla J_{io}\left(\mathbf{S}_i\right) \\ &\times\left(\mathrm{H_i}\left(\mathbf{S}_i\right) + G_i U_i^*\right) + {}^C\mathrm{D}_{0,t}^{\alpha}V_4\left(t\right) \\ &\le -\mathfrak{M}_i^T\mathbb{S}_i\mathfrak{M}_i + \mathfrak{M}_i^T\mathbb{F}_i - \frac{1}{2}\tilde{\phi}_{\mathrm{in}}^T\sum\left(\mathbf{S}_i, \hat{U}_i\right)\nabla\xi_{\mathrm{in}}\hbar_i\nabla J_{io}\left(\mathbf{S}_i\right) \\ &+ \nabla J_{io}\left(\mathbf{S}_i\right)\left(\mathrm{H_i}\left(\mathbf{S}_i\right) + G_i U_i^*\right) + {}^C\mathscr{D}_{0,t}^{\alpha}V_4\left(t\right)\end{aligned} \tag{69}$$

where

$$\mathfrak{M}_i \equiv \left[\tilde{\phi}_{\mathrm{in}}^T\varphi_{\mathrm{in}}, \tilde{\phi}_{\mathrm{in}}^T\right]^T, \quad \mathbb{S}_i \equiv \begin{bmatrix}1 & -\frac{1}{2}F_{\mathrm{in}_1}^T \\ -\frac{1}{2}F_{\mathrm{in}_1} & F_{\mathrm{in}_2} - \frac{1}{2}\frac{\varphi_{\mathrm{in}}}{\underline{m}_{\mathrm{in}}}\phi_{\mathrm{in}}^T\bar{D}_i\end{bmatrix}$$

$$\mathbb{F}_i \equiv \begin{bmatrix}-e_{i_{\mathrm{HJB}}}/\underline{m}_{\mathrm{in}} \\ \left(F_{\mathrm{in}_2} - F_{\mathrm{in}_1}\varphi_{\mathrm{in}}^T - \frac{\varphi_{\mathrm{in}}}{4\underline{m}_{\mathrm{in}}}\phi_{\mathrm{in}}^T\bar{D}_i\right)\phi_{\mathrm{in}}\end{bmatrix}.$$

$$\bar{\mathrm{G}}_i^* i = \begin{bmatrix}\bar{\beta}_i^*\mathbf{I} & 0 & 0 \\ 0 & \mathbf{I} & \left(-F_{\mathrm{in}_1}/2 - \bar{D}_i\phi_{\mathrm{in}}/8\underline{m}_{\mathrm{in}}\right)^T \\ 0 & -\frac{F_{\mathrm{in}_1}}{2} - \frac{\bar{D}_i\phi_{\mathrm{in}}}{8\underline{m}_{\mathrm{in}}} & F_{\mathrm{in}_2} - \frac{1}{8}\left(\bar{D}_i\phi_{\mathrm{in}}(\underline{m}_{\mathrm{in}}\varphi_{\mathrm{in}})^T + \underline{m}_{\mathrm{in}}\varphi_{\mathrm{in}}\phi_{\mathrm{in}}^T\bar{D}_i\right)\end{bmatrix}$$

Substituting (49) and (61) into (69) yields

$$
\begin{aligned}
{}^{C}\mathscr{D}_{0,t}^{\alpha}V\left(t\right) \leq & -\lambda_{\min}\left(\mathbb{S}_i\right)\left\|\mathfrak{M}_i\right\|^2+\left\|\mathfrak{M}_i\right\|\left\|\mathbb{F}_i\right\|-\frac{3}{2}\mathbf{g}_o\left\|\tilde{\lambda}_o\right\|^2 \\
& +\Xi_i-\left(\mathbf{k}_o-\frac{\psi^2}{2}\right)\left\|\mathbf{S}_i\right\|^2-\frac{1}{2}\tilde{\phi}_{\mathrm{in}}^{T}\sum\left(\mathbf{S}_i,\hat{U}_i\right)\nabla\xi_{\mathrm{in}}\hbar_i\nabla J_{io}(\mathbf{S}_i) \\
& +\frac{1}{2}c_{io}^2\left\|\mathbf{S}_i\right\|+\nabla J_{io}(\mathbf{S}_i)^{C}\mathscr{D}_{0,t}^{\alpha}\mathbf{S}_i \qquad (70)
\end{aligned}
$$

where $\lambda_{\min}(\mathbb{S}_i)$ denotes the minimum eigenvalue of $\mathbb{S}_i, \mathbf{k}_o=\min(k_{1i},k_{2i},k_{3i},k_{4i}),\quad \mathbf{g}_o=\min(g_{2i},g_{4i}),$ and $\lambda_o\equiv[\lambda_{2i},\lambda_{4i}]^T$.

*Case 1:* $\sum\left(\mathbf{S}_i,\hat{U}_i\right)=0$. It has a positive constant $\Phi_s$ such that $\Phi_s<\left\|\mathbf{S}_i\right\|$ since $\nabla J_{io}(\mathbf{S}_i)^{C}\mathscr{D}_{0,t}^{\alpha}\mathbf{S}_i<0$. Then (70) is rewritten as

$$
\begin{aligned}
{}^{C}\mathscr{D}_{0,t}^{\alpha}V\left(t\right) \leq & -\lambda_{\min}\left(\mathbb{S}_i\right)\left(\left\|\mathfrak{M}_i\right\|-\frac{1}{2\lambda_{\min}\left(\mathbb{S}_i\right)}\left\|\mathbb{F}_i\right\|\right)^2 \\
& -\frac{3}{2}\mathbf{g}_o\left\|\tilde{\lambda}_o\right\|^2-\left(\mathbf{k}_o-\psi^2/2\right)\left(\left\|\mathbf{S}_i\right\|-\frac{c_{io}^2}{2\mathbf{k}_o-\psi^2}\right)^2 \\
& -\Phi_s\left\|\nabla J_{io}\left(\mathbf{S}_i\right)\right\|+\Upsilon_s \qquad (71)
\end{aligned}
$$

where

$$
\Upsilon_s=\frac{\left\|\mathbb{F}_i\right\|^2}{4\lambda_{\min}\left(\mathbb{S}_i\right)}+\frac{c_{io}^4}{16\mathbf{k}_o-8\psi^2}+\Xi_i.
$$

To ensure the stability of the closed-loop system, ${}^{C}\mathscr{D}_{0,t}^{\alpha}V(t)\leq 0$ only when

$$
\left\|\nabla J_{io}\left(\mathbf{S}_i\right)\right\|\geq\Upsilon_s/\Phi_s=\mathbf{A}_1 \qquad (72)
$$

or

$$
\left\|\mathfrak{M}_i\right\|\geq\sqrt{\Upsilon_s/\lambda_{\min}\left(\mathbb{S}_i\right)}+\left\|\mathbb{F}_i\right\|/2\lambda_{\min}\left(\mathbb{S}_i\right)=\mathbf{B}_1 \qquad (73)
$$

or

$$
\left\|\tilde{\boldsymbol{\lambda}}_o\right\|\geq\sqrt{2\Upsilon_s/3\mathbf{g}_o}=\mathbf{C}_1 \qquad (74)
$$

or

$$
\left\|\mathbf{S}_i\right\|\geq\sqrt{\Upsilon_s/\left(\mathbf{k}_o-\psi^2/2\right)}+\frac{c_{io}^2}{2\mathbf{k}_o-\psi^2}=\mathbf{D}_1. \qquad (75)
$$

*Case 2:* $\sum\left(\mathbf{S}_i,\hat{U}_i\right)=1$. There exists the relation as $U_i^*-\hat{U}_i=-\frac{1}{2}R_i^{-1}G_i^T(\nabla\boldsymbol{\xi}_{\mathrm{in}}^T(\mathbf{S}_i)\tilde{\phi}_{\mathrm{in}}+\nabla\varepsilon_{\mathrm{in}}(\mathbf{S}_i))$.

Then (70) is rewritten as

$$
\begin{aligned}
{}^{C}\mathrm{D}_{0,t}^{\alpha}V\left(t\right) \leq & -\lambda_{\min}\left(\mathbb{S}_i\right)\left(\left\|\mathfrak{M}_i\right\|-\frac{\left\|\mathbb{F}_i\right\|}{2\lambda_{\min}\left(\mathbb{S}_i\right)}\right)^2 \\
& -\frac{3}{2}\mathbf{g}_o\left\|\tilde{\lambda}_o\right\|^2-\lambda_{\min}\left(\Lambda_i\left(\mathbf{S}_i\right)\right) \\
& \times\left(\left\|\nabla J_{io}\left(\mathbf{S}_i\right)\right\|-\frac{\hbar_{\max}\varepsilon_s}{4\lambda_{\min}\left(\Lambda_i\left(\mathbf{S}_i\right)\right)}\right)^2 \\
& -\left(\mathbf{k}_o-\frac{\psi^2}{2}\right)\cdot\left(\left\|\mathbf{S}_i\right\|-\frac{c_{io}^2}{\left(2\mathbf{k}_o-\psi^2\right)}\right)^2+\Upsilon_o \qquad (76)
\end{aligned}
$$

where $\|\nabla\varepsilon_{\mathrm{in}}\|\leq\varepsilon_s$, $\lambda_{\min}(\Lambda_i(\mathbf{S}_i))$ is the minimum eigenvalue of $\Lambda_i(\mathbf{S}_i)$,$\Upsilon_o=\frac{\hbar_{\max}^2\varepsilon_s^2}{16\lambda_{\min}(\Lambda_i(\mathbf{S}_i))}+\frac{\|\mathbb{F}_i\|^2}{4\lambda_{\min}(\mathbb{S}_i)}+\frac{c_{io}^4}{16\mathbf{k}_o-8\psi^2}+\Xi_i$, and $\|\hbar_i\|\leq\hbar_{\max}$.

If the following condition holds:

$$
\left\|\nabla J_{io}\left(\mathbf{S}_i\right)\right\|\geq\sqrt{\Upsilon_o/\lambda_{\min}\left(\Lambda_i\left(\mathbf{S}_i\right)\right)}+\frac{\hbar_{\max}\varepsilon_s}{4\lambda_{\min}\left(\Lambda_i\left(\mathbf{S}_i\right)\right)}=\mathbf{A}_2 \qquad (77)
$$

or

$$
\left\|\mathfrak{M}_i\right\|\geq\sqrt{\Upsilon_o/\lambda_{\min}\left(\mathbb{S}_i\right)}+\left\|\mathbb{F}_i\right\|/2\lambda_{\min}\left(\mathbb{S}_i\right)=\mathbf{B}_2 \qquad (78)
$$

or

$$
\left\|\tilde{\lambda}_o\right\|\geq\sqrt{2\Upsilon_o/3\mathbf{g}_o}=\mathbf{C}_2 \qquad (79)
$$

or

$$
\left\|\mathbf{S}_i\right\|\geq\sqrt{\Upsilon_o/\left(\mathbf{k}_o-\psi^2/2\right)}+\frac{c_{io}^2}{2\mathbf{k}_o-\psi^2}=\mathbf{D}_2 \qquad (80)
$$

then ${}^{C}\mathrm{D}_{0,t}^{\alpha}V(t)\leq 0$.

From Cases 1 and 2, it can be drawn that ${}^{C}\mathscr{D}_{0,t}^{\alpha}V(t)\leq 0$ since $\|\mathfrak{M}_i\|\geq\max(\mathbf{B}_1,\mathbf{B}_2)$,$\|\tilde{\boldsymbol{\lambda}}_o\|\geq\max(\mathbf{C}_1,\mathbf{C}_2)$, $\|\mathbf{S}_i\|\geq\max(\mathbf{D}_1,\mathbf{D}_2)$ or $\|\nabla J_{io}(\mathbf{S}_i)\|\geq\max(\mathbf{A}_1,\mathbf{A}_2)$.

## VI. Simulation Results and Discussion

In this section, to demonstrate the effectiveness of the presented method above, the simulation of accelerated adaptive fuzzy optimal control for three coupled fractional-order electromechanical transducers is carried out. The reference signals are given as $x_{L_1}=1.5\sin 2t$ and $x_{L_3}=0.2\sin 2t$ here. The parameters for the speed function are set to $\mathbf{T}=1$ and $b_\psi=0.5$. According to Theorem 1, the design parameters of the feedforward fuzzy controller are chosen to be$k_{1i}=35$, $k_{2i}=55$, $k_{3i}=12$, $k_{4i}=25$, $\mu_{2i}=\mu_{4i}=4$, $g_{2i}=g_{4i}=5$, and $B_{2i}=B_{4i}=1$. The regulation parameters of the TD are set to $\vartheta_{1i}=\vartheta_{3i}=4$ and $\sigma_{1i}=\sigma_{3i}=0.3$. Besides, the upper and lower widths of the MFs for the RNT2SFNN are selected as $\bar{\sigma}_{\tilde{A}_j^i}=0.08$, $\bar{\sigma}_{\tilde{B}_j}=0.06$, $\underline{\sigma}_{\tilde{A}_j^i}=0.02$, and $\underline{\sigma}_{\tilde{B}_j}=0.01$. The centers of the MFs and the corresponding parameter are defined as $[-0.8\ -0.5\ 0\ 0.5\ 0.8]$ and $r=0.06$. The time delays are chosen as $\tau_{1i}=0.03\sin t$ and $\tau_{3i}=0.01\sin 0.4t$.

The penalty function associated with the optimal feedback control is $Q_i(\mathbf{S}_i)=\sum_{j=1}^{4}S_{ji}^2$. The design parameters of the adaptive optimal feedback controller are set to be $a_{in}=5$, $F_{\mathrm{in}_1}=[0202]^T$, $F_{\mathrm{in}_2}=\mathrm{diag}\{0\ 3\ 0\ 3\}$, and $R=\mathbf{I}_{4\times 4}$.

Fig. 6 exhibits the tracking trajectories between the reference signals and actual signals for three coupled electromechanical transducers. Four curves overlap each other in two subgraphs. It is very obvious that the system states can track the reference signals quickly with very tiny errors in a short time. Meanwhile, the synchronization for a small network of three coupled electromechanical transducers is achieved and chaotic oscillations of the electromechanical transducers are completely suppressed in contrast with Fig. 2–4 in a very short time.

Fig. 7 shows the adaptive laws of the RNT2SFNN in the feedforward controller and updated laws of the actor/critic RNT2SFNN in the optimal controller for three coupled electromechanical transducers. All curves converge quickly to a stable value once the proposed scheme gets involved. It can be concluded that all unknown system dynamics can be better compensated by the RNT2SFNN within a short time. It also

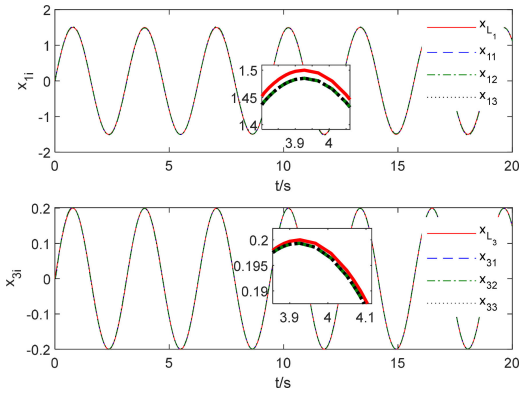


Fig. 6. Tracking performance between the reference signals and actual signals.

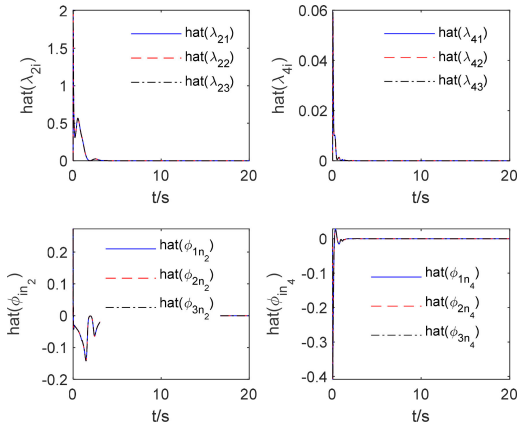


Fig. 7. Adaptive laws of the RNT2SFNN in the feedforward controller and optimal controller.

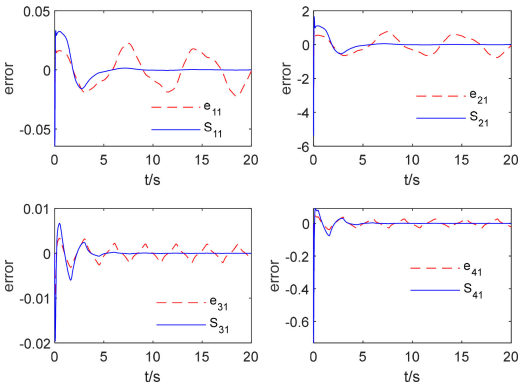


Fig. 8. Accelerated convergence performance for the tracking errors of the first fractional-order electromechanical transducer.

reveals that the results of synchronization for three coupled electromechanical transducers are satisfactory in the presence of chaotic oscillation, time delay, and coupling configuration.

Fig. 8 presents the accelerated convergence performance for the tracking errors and accelerated errors. The stabilization time and fluctuation amplitude of $S_{j1}$ are obviously smaller than $e_{j1}$. It can also be seen that all error variables have a rapid convergence with a very litter fluctuate. The proposed scheme can obtain better performance at an assignable decay rate by using the speed function. Fig. 9 presents the approximation performance for the designed fractional-order TD under

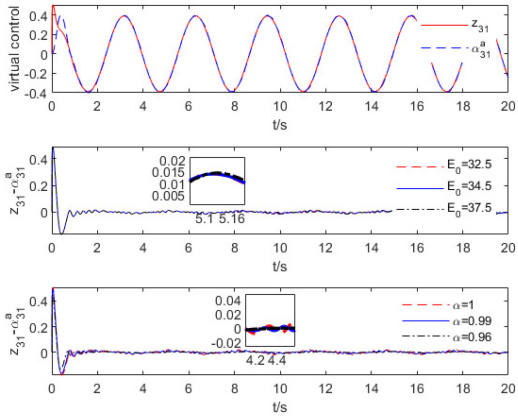


Fig. 9. Approximation performance for the fractional-order TD under different conditions.

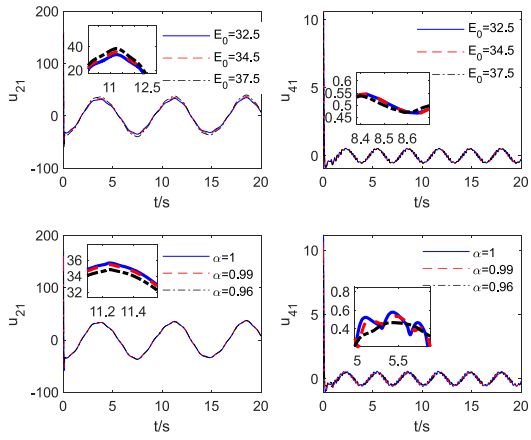


Fig. 10. Whole control inputs including the feedforward controller and optimal controller under different conditions.

different fractional orders and external excitations. It is very obvious that the fractional-order TD can approximate unknown signals with very high precision. Meanwhile, the output signal of the fractional-order TD is not sensitive to the fluctuations of fractional order and external excitation. Fig. 10 shows the control inputs of the feedforward controller and optimal controller. The control inputs can be bounded in a region and remain stable in very short time, although there exist the changes of fractional order and external excitation. Fig. 11 depicts the curve of the residual error associated with the HJB equation. It is clear that the error approaches zero 2.5 s later and the proposed scheme runs in an optimal manner. Several curves of the Figs. 9–11 overlap under different conditions. It further illustrates that the presented scheme has good antidisturbance ability and toughness.

## VII. Conclusion

This article developed an accelerated adaptive fuzzy optimal control method for a small network of coupled fractional-order electromechanical transducers in the presence of chaotic oscillation, unknown dynamics, and time delays that can be used for loading in assembly line works, scaling up manufacturing processes, and controlling parallel operating systems, intestinal

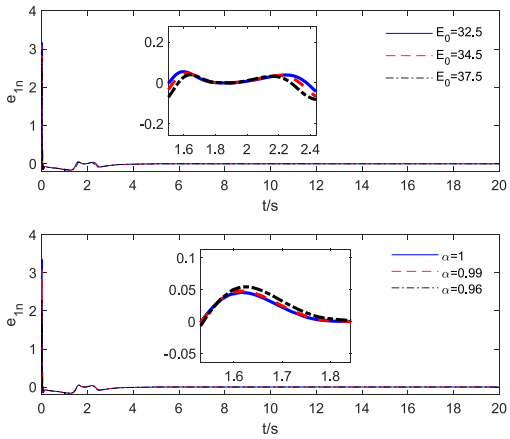


Fig. 11. Residual error associated with the HJB equation under different conditions.

motions, colorectal myoelectrical activities, and pattern generators. The mathematical model of three coupled electromechanical transducers with nearest-neighbor coupling configuration was constructed. The dynamical analysis revealed that its dynamical behaviors were related closely to external excitations and fractional orders. The real control strategy was made up of a feedforward controller fusing with the RNT2SFNN, TD, and speed function on the basis of the backstepping control and a feedback controller integrating with the RNT2SFNN and PI under an actor/critic structure to obtain the Nash equilibrium of the corresponding HJB equation. The stability of the closed-loop system was proved by using the fractional-order Lyapunov function and the optimal control problem mentioned above was well solved. In future work, we plan to focus more on the prescribed performance fuzzy optimal control of coupled electromechanical systems based on the data-driven adaptive critic method.

## REFERENCES


[1] S. Boccaletti, V. Latora, Y. Moreno, M. Chavez, and D.-U. Hwang, "Complex networks: Structure and dynamics," *Phys. Rep.*, vol. 424, no. 4/5, pp. 175–308, 2006.

[2] G. S. M. Ngueuteu, R. Yamapi, and P. Woafo, "Stability of synchronized network of chaotic electromechanical devices with nearest and all-to-all couplings," *J. Sound Vib.*, vol. 318, no. 4, pp. 1119–1138, 2008.

[3] G. S. M. Ngueuteu and P. Woafo, "Dynamics and synchronization analysis of coupled fractional-order nonlinear electromechanical systems," *Mech. Res. Commun.*, vol. 46, no. 4, pp. 20–25, 2012.

[4] M. Wissler and E. Mazza, "Electromechanical coupling in dielectric elastomer actuators," *Sensor Actuator A, Phys.*, vol. 138, no. 2, pp. 384–393, 2007.

[5] G.-W. Deng *et al.*, "Strongly coupled nanotube electromechanical resonators," *Nano Lett.*, vol. 16, no. 9, pp. 5456–5462, 2016.

[6] Z. Su, Y. Li, and G. Yang, "Dietary composition perception algorithm using social robot audition for mandarin Chinese," *IEEE Access*, vol. 8, pp. 8768–8782, 2020.

[7] H. M. Ouakad, A. H. Nayfeh, S. Choura, and F. Najar, "Nonlinear feedback controller of a microbeam resonator," *J. Vib. Control*, vol. 21, no. 9, pp. 1680–1697, 2015.

[8] T. Haidegger, L. Kovács, S. Preitl, R. E. Precup, B. Benyo, and Z. Benyó, "Controller design solutions for long distance telesurgical applications," *Int. J. Artif. Intell.*, vol. 6, no. 11 S, pp. 48–71, 2011.

[9] S. Luo, F. L. Lewis, Y. Song, and K. G. Vamvoudakis, "Adaptive backstepping optimal control of a fractional-order chaotic magnetic-field electromechanical transducer," *Nonlinear Dyn.*, doi: 10.1007/s11071-020-05518-5, to be published.

[10] M. Pérez-Molina and M. F. Pérez-Polo, "Fold-Hopf bifurcation, steady state, self-oscillating and chaotic behavior in an electromechanical transducer with nonlinear control," *Commun. Nonlinear Sci. Numer. Simul.*, vol. 17, no. 12, pp. 5172–5188, 2012.

[11] G. S. M. Ngueuteu, R. Yamapi, and P. Woafo, "Effects of higher nonlinearity on the dynamics and synchronization of two coupled electromechanical devices," *Commun. Nonlinear Sci. Numer. Simul.*, vol. 13, no. 7, pp. 1213–1240, 2008.

[12] M. P. Aghababa, "A fractional sliding mode for finite-time control scheme with application to stabilization of electrostatic and electromechanical transducers," *Appl. Math. Model.*, vol. 39, no. 20, pp. 6103–6113, 2015.

[13] X. Cao, P. Shi, Z. Li, and M. Liu, "Neural-network-based adaptive backstepping control with application to spacecraft attitude regulation," *IEEE Trans. Neural Netw. Learn. Syst.*, vol. 29, no. 9, pp. 4303–4313, Sep. 2018.

[14] Y.-J. Liu, Y. Gao, S. Tong, and Y. Li, "Fuzzy approximation-based adaptive backstepping optimal control for a class of nonlinear discrete-time systems with dead-zone," *IEEE Trans. Fuzzy Syst.*, vol. 24, no. 1, pp. 16–28, Feb. 2016.

[15] Y. Song, Z. Shen, L. He, and X. Huang, "Neuroadaptive control of strict feedback systems with full-state constraints and unknown actuation characteristics: An inexpensive solution," *IEEE Trans. Cybern.*, vol. 48, no. 11, pp. 3126–3134, Nov. 2018.

[16] K. Zhao, Y. Song, and Z. Shen, "Neuroadaptive fault-tolerant control of nonlinear systems under output constraints and actuation faults," *IEEE Trans. Neural Netw. Learn. Syst.*, vol. 29, no. 2, pp. 286–298, Feb. 2018.

[17] Y. Li, K. Sun, and S. Tong, "Observer-based adaptive fuzzy fault-tolerant optimal control for SISO nonlinear systems," *IEEE Trans. Cybern.*, vol. 49, no. 2, pp. 649–661, Feb. 2019.

[18] R. Sepulveda, O. H. Montiel Ross, O. Castillo, and P. Melin, "Modelling and simulation of the defuzzification stage of a type-2 fuzzy controller using VHDL code," *Contr. Intell. Syst.*, vol. 39, no. 1, pp. 33–40, 2011.

[19] R.-E. Precup, M.-L. Tomescu, and C.-A. Dragos, "Stabilization of Rössler chaotic dynamical system using fuzzy logic control algorithm," *Int. J. Gen. System.*, vol. 43, no. 5, pp. 413–433, 2014.

[20] L. Maciel, F. Gomide, and R. Ballini, "Enhanced evolving participatory learning fuzzy modeling: An application for asset returns volatility forecasting," *Evolving Syst.*, vol. 5, no. 2, pp. 75–88, 2014.

[21] C. P. Chen, G.-X. Wen, Y.-J. Liu, and Z. Liu, "Observer-based adaptive backstepping consensus tracking control for high-order nonlinear semi-strict-feedback multiagent systems," *IEEE Trans. Cybern.*, vol. 46, no. 7, pp. 1591–1601, Jul. 2016.

[22] J. Sun and C. Liu, "Distributed fuzzy adaptive backstepping optimal control for nonlinear multi-missile guidance systems with input saturation," *IEEE Trans. Fuzzy Syst.*, vol. 27, no. 3, pp. 447–461, Mar. 2019.

[23] D. Ding, D. Qi, J. Peng, and Q. Wang, "Asymptotic pseudo-state stabilization of commensurate fractional-order nonlinear systems with additive disturbance," *Nonlinear Dyn.*, vol. 81, no. 1–2, pp. 667–677, 2015.

[24] H. Heydarinejad, H. Delavari, and D. Baleanu, "Fuzzy type-2 fractional backstepping blood glucose control based on sliding mode observer," *In. J. Dyn. Control*, vol. 7, no. 1, pp. 341–354, 2018.

[25] H. Liu, S. Li, H. Wang, and Y. Sun, "Adaptive fuzzy control for a class of unknown fractional-order neural networks subject to input nonlinearities and dead-zones," *Inform. Sci.*, vol. 454/455, pp. 30–45, 2018.

[26] H. Liu, Y. Pan, S. Li, and Y. Chen, "Adaptive fuzzy backstepping control of fractional-order nonlinear systems," *IEEE Trans. Syst. Man Cybern. Syst.*, vol. 47, no. 8, pp. 2209–2217, Aug. 2017.

[27] D. Sheng, Y. Wei, S. Cheng, and W. Yong, "Observer-based adaptive backstepping control for fractional order systems with input saturation," *ISA Trans.*, vol. 82, pp. 18–29, 2018.

[28] Y. Wei, P. W. Tse, Z. Yao, and Y. Wang, "Adaptive backstepping output feedback control for a class of nonlinear fractional order systems," *Nonlinear Dyn.*, vol. 86, no. 2, pp. 1047–1056, 2016.

[29] C. P. Bechlioulis and G. A. Rovithakis, "Robust adaptive control of feedback linearizable MIMO nonlinear systems with prescribed performance," *IEEE Trans. Automat Contr.*, vol. 53, no. 9, pp. 2090–2099, Oct. 2008.

[30] Y. Yang, J. Tan, and D. Yue, "Prescribed performance tracking control of a class of uncertain pure-feedback nonlinear systems with input saturation," *IEEE Trans. Syst. Man Cybern. Syst.*, vol. 50, no. 5, pp. 1733–1745, May 2020.

[31] Y. Song and K. Zhao, "Accelerated adaptive control of nonlinear uncertain systems," in *Proc. Amer. Control Conf.*, 2017, pp. 2471–2476.

[32] H. Modares, F. L. Lewis, and Z. P. Jiang, "H ∞ tracking control of completely unknown continuous-time systems via off-policy reinforcement learning," *IEEE Trans. Neural Netw. Learn. Syst.*, vol. 26, no. 10, pp. 2550–2562, Oct. 2015.

[33] K. G. Vamvoudakis and F. L. Lewis, "Multi-player non-zero-sum games: Online adaptive learning solution of coupled Hamilton–Jacobi equations," *Automatica*, vol. 47, no. 8, pp. 1556–1569, 2011.
[34] K. G. Vamvoudakis and F. L. Lewis, "Online actor–critic algorithm to solve the continuous-time infinite horizon optimal control problem," *Automatica*, vol. 46, no. 5, pp. 878–888, 2010.
[35] D. Vrabie and F. Lewis, "Neural network approach to continuous-time direct adaptive optimal control for partially unknown nonlinear systems," *Neural Netw.*, vol. 22, no. 3, pp. 237–246, 2009.
[36] S. Luo, J. Li, S. Li, and J. Hu, "Dynamical analysis of the fractional-order centrifugal flywheel governor system and its accelerated adaptive stabilization with the optimality," *Int. J. Elect. Power Energy Syst.*, vol. 118, 2020, Art. no. 105792.
[37] S. Luo, S. Li, and F. Tajaddodianfar, "Chaos and adaptive control of the fractional-order magnetic-field electromechanical transducer," *Int. J. Bifurcation Chaos*, vol. 27, no. 13, 2018, Art. no. 1750203.
[38] H. Zargarzadeh, T. Dierks, and S. Jagannathan, "Optimal control of nonlinear continuous-time systems in strict-feedback form," *IEEE Trans. Neural Netw. Learn. Syst.*, vol. 26, no. 10, pp. 2535–2549, Oct. 2015.
[39] K. Sun, Y. Li, and S. Tong, "Fuzzy adaptive output feedback optimal control design for strict-feedback nonlinear systems," *IEEE Trans. Syst. Man Cybern. Syst.*, vol. 47, no. 1, pp. 33–44, Jan. 2017.
[40] K. G. Vamvoudakis, H. Modares, B. Kiumarsi, and F. L. Lewis, "Game theory-based control system algorithms with real-time reinforcement learning: How to solve multiplayer games online," *IEEE Control Syst. Mag.*, vol. 37, no. 1, pp. 33–52, Feb. 2017.
[41] H. Modares and F. L. Lewis, "Optimal tracking control of nonlinear partially-unknown constrained-input systems using integral reinforcement learning," *Automatica*, vol. 50, no. 7, pp. 1780–1792, 2014.
[42] K. G. Vamvoudakis and J. P. Hespanha, "Cooperative q-learning for rejection of persistent adversarial inputs in networked linear quadratic systems," *IEEE Trans. Autom. Contr.*, vol. 63, no. 4, pp. 1018–1031, Apr. 2018.
[43] P. Zhou, R. J. Bai, and J. M. Zheng, "Stabilization of a fractional-order chaotic brushless DC motor via a single input," *Nonlinear Dyn.*, vol. 82, no. 1/2, pp. 519–525, 2015.
[44] J. S. K., S. Effati, and M. Pakdaman, "A neural network approach for solving a class of fractional optimal control problems," *Neural Process. Lett.*, vol. 45, no. 1, pp. 59–74, 2017.
[45] M. Wang, B. Chen, and P. Shi, "Adaptive neural control for a class of perturbed strict-feedback nonlinear time-delay systems," *IEEE Trans. Syst. Man Cybern. Syst.*, vol. 38, no. 3, pp. 721–730, Jun. 2008.
[46] A. Mohammadzadeh and S. Ghaemi, "Robust synchronization of uncertain fractional-order chaotic systems with time-varying delay," *Nonlinear Dyn.*, vol. 93, pp. 1809–1821, 2018.
[47] K. Zhao, Y. Song, T. Ma, and L. He, "Prescribed performance control of uncertain Euler-Lagrange systems subject to full-state constraints," *IEEE Trans. Neural Netw. Learn. Syst.*, vol. 29, no. 8, pp. 3478–3489, Aug. 2018.
[48] X. Huang, Y. Song, and J. Lai, "Neuro-adaptive control with given performance specifications for strict feedback systems under full-state constraints," *IEEE Trans. Neural Netw. Learn. Syst.*, vol. 30, no. 1, pp. 25–34, Jan. 2019.
[49] S. Luo and Y. Song, "Chaos analysis-based adaptive backstepping control of the microelectromechanical resonators with constrained output and uncertain time delay," *IEEE Trans. Ind. Electron.*, vol. 63, no. 10, pp. 6217–6225, Oct. 2016.
[50] Y. Wei, Y. Chen, S. Liang, and Y. Wang, "A novel algorithm on adaptive backstepping control of fractional order systems," *Neurocomputing*, vol. 165, pp. 395–402, 2015.

**Shaohua Luo** received the B.S., M.S., and Ph.D. degrees in mechanical engineering from Chongqing University, Chongqing, China, in 2005, 2009, and 2014, respectively.

He was involved in postdoctoral research with Chongqing University from 2014 to 2016 in the area of adaptive control and chaos control of nonlinear systems. He is currently a Professor with the School of Mechanical Engineering, Guizhou University, Guiyang, China. His current research interests include the fractional-order electromechanical systems, mechanical and electrical transmission control, dynamic analysis, adaptive control, and chaos control of nonlinear systems.

**Frank L. Lewis** (Fellow, IEEE) received the bachelor's degree in physics/electrical engineering and the M.S.E.E. degree in electrical engineering from Rice University, Houston, TX, USA, in 1971 the M.S. degree in aeronautical engineering from the University of West Florida, Pensacola, FL, USA, in 1977 and the Ph.D. degree in electrical engineering from the Georgia Institute of Technology, Atlanta, GA, USA, in 1981.

He is currently a Distinguished Scholar Professor and a Distinguished Teaching Professor with the University of Texas at Arlington, Arlington, TX, USA, and the Moncrief-ODonnell Chair of the University of Texas at Arlington Research Institute. He has authored six U.S. patents, numerous journal special issues, journal papers, and 20 books, including *Optimal Control*, *Aircraft Control*, *Optimal Estimation*, and *Robot Manipulator Control*. His current research interests involve in feedback control, intelligent systems, cooperative control systems, and nonlinear systems.

Prof. Lewis is a Member of the National Academy of Inventors, Fellow of the International Federation of Automatic Control and the Institute of Measurement and Control, U.K., Texas Board of Professional Engineer, U.K. Chartered Engineer, and Founding Member of the Board of Governors of the Mediterranean Control Association. He was a recipient of the Fulbright Research Award, NSF Research Initiation Grant, Terman Award from the American Society for Engineering Education, Gabor Award from the International Neural Network Society, Honeywell Field Engineering Medal from the Institute of Measurement and Control, U.K., Neural Networks Pioneer Award from the IEEE Computational Intelligence Society, Outstanding Service Award from the Dallas IEEE Section, and Texas Regents Outstanding Teaching Award in 2013. He was elected as an Engineer of the year by the Fort Worth IEEE Section. He was listed in the Fort Worth Business Press Top 200 Leaders in Manufacturing.

**Yongduan Song** (Fellow, IEEE) received the Ph.D. degree in electrical and computer engineering from Tennessee Technological University, Cookeville, TN, USA, in 1992.

He was a tenured Full Professor with North Carolina A&T State University, Greensboro, NC, USA, from 1993 to 2008 and a Langley Distinguished Professor with the National Institute of Aerospace, Hampton, VA, USA, from 2005 to 2008. He is currently the Dean of the School of Automation and the Founding Director of the Institute of Smart Systems and Renewable Energy, Chongqing University, Chongqing, China. He was one of the six Langley Distinguished Professors with the National Institute of Aerospace (NIA), Founding Director of Cooperative Systems at NIA. He has served as an Associate Editor/Guest Editor for several prestigious scientific journals. His current research interests include intelligent systems, guidance navigation and control, bio-inspired adaptive and cooperative systems, rail traffic control and safety, and smart grid.

Prof. Song was a recipient of several competitive research awards from the National Science Foundation, National Aeronautics and Space Administration, U.S. Air Force Office, U.S. Army Research Office, and U.S. Naval Research Office.

**Hassen M. Ouakad** (Member, IEEE) received the B.S., M.S., and Ph.D. degrees in mechanical engineering from Tunisia Polytechnic School, Virginia Polytechnic Institute and State University, Blacksburg, VA, USA, and State University of New York, Binghamton, NY, USA, in 2007, 2008 and 2010, respectively.

He was involved in postdoctoral research with Texas A&M University, Doha, Qatar from 2010 to 2012 in the linear/nonlinear dynamics, system control, and mechatronics. He is currently an Associate Professor of Mechanical and Industrial Engineering Department, Sultan Qaboos University, Muscat, Oman, where he currently heads the System Dynamics and Control Laboratory.

Dr. Ouakad was the recipient of the 2010 and 2018 Excellence in Research Award granted by the State University of New York at Binghamton and KFUPM. He authored about 90 papers and serves as an Associate Editor for several prestigious scientific journals.